File – research report

1122

POST-ELASTIC ANALYSIS OF A WEB CONNECTION IN DIRECT TENSION

BY

SUBHASH C. ANAND
PROFESSOR OF CIVIL ENGINEERING

author

key words:
1. Web Connections
2. Connections
3. Plate Connections

AND

RICHARD FREDRICK BERTZ
GRADUATE STUDENT

DEPARTMENT OF CIVIL ENGINEERING
CLEMSON UNIVERSITY

AUGUST 1980

2S-80

00314

AMERICAN INSTITUTE OF STEEL CONSTRUCTION, INC.
The Wrigley Building / 400 North Michigan Avenue / Chicago, Illinois 60611 / 312 • 670-2400

File

'79 FELLOWSHIP REPORT

October 27, 1980

Clemson University
College of Engineering
Clemson, SC 29631

ATTENTION: Professor Subhash C. Anand
Department of Civil Engineering

Dear Mr. Anand:

Thank you for sending us copies of the M. S. Thesis entitled "Post-Elastic Analysis of a Web Connection in Direct Tension". It is a fine piece of work.

Mr. Richard Bertz and yourself are to be commended for this research effort and congratulated for receiving the First Award in the Graduate Division (Structures) of the 1980 Engineering Student Design Competition of the James F. Lincoln Arc Welding Foundation.

AISC is pleased that its financial assistance contributed to such a successful research study. Good luck in your future work.

Cordially,

Nestor Iwankiw

Nestor R. Iwankiw
Asst. Director of Engineering
Research and Education

NRI/cp

00315

College of Engineering
DEPARTMENT OF CIVIL ENGINEERING

CLEMSON UNIVERSITY

September 25, 1980

AISC Education Foundation
American Institute of Steel Construction
The Wrigley Building
400 North Michigan Avenue
Chicago, IL 60611

Dear Sir:

Enclosed please find two copies of a M.S. Thesis, entitled "Post-Elastic Analysis of a Web Connection in Direct Tension," that was submitted by Mr. Richard F. Bertz to the Graduate School at Clemson University as a partial fulfillment for the degree of Master of Science in Civil Engineering. This research was carried out by Mr. ~~Bertz at~~ Clemson while he was being supported by the 1979 AISC Fellowship Award.

I would like to mention here that the research presented in this report was submitted by Mr. Bertz for consideration in the 1980 Engineering Student Design Compitition of the James F. Lincoln Arc Welding Foundation, and has been granted the First Award in the Graduate Division (Structures). Clemson University is quite proud of the excellent work done by Mr. Richard F. Bertz.

Clemson University wishes to express its sincere thanks to the American Institute of Steel Construction for granting a 1979 AISC Fellowship to Mr. Bertz to study at Clemson, without which the research reported in the enclosed copies would not have been possible.

Sincerely yours,

SCAnand

Subhash C. Anand
Professor
of Civil Engineering and
Faculty Advisor
to Richard F. Bertz

SCA/ms

enclosures

August 1, 1980

To the Graduate School:

Herewith is submitted a thesis written by Richard Fredrick Bertz entitled "Post-Elastic Analysis of a Web Connection in Direct Tension." I recommend that it be accepted in partial fulfillment of the requirements for the degree of Master of Science, with a major in Civil Engineering.

E. C. Anand

Thesis Advisor

We have reviewed this thesis and recommend its acceptance:

Michael L. Morrell

Russell H. Brown

Accepted for the Graduate School:

Farrell L. Brown

POST-ELASTIC ANALYSIS OF A WEB CONNECTION IN DIRECT TENSION

A Thesis

Presented to

the Graduate School of

Clemson University

In Partial Fulfillment

of the Requirements for the Degree

Master of Science

Civil Engineering

---

by

Richard Fredrick Bertz

August 1980

ABSTRACT

Light bracing composed of a tension plate welded to the web of a column or beam section is employed quite often in the design of steel structures. Generally, the strength of the web in carrying the tensile load is of primary concern. There are two analysis procedures which have been suggested for the strength analysis of the web. The first is an elastic method suggested by Blodgett, and the second, an ultimate strength yield line method proposed by Kapp.

Experimental tests of these connections have indicated that the strength of these connections are, in general, much greater than the strength predicted by either the elastic or the yield line theories. A post-elastic analysis is conducted in this study using the finite element technique to determine the elastic-plastic behavior of this type of connection.

An evaluation of the data generated by a computer model using a plate bending element developed in this paper indicates that yielding in the web develops in broad regions, and not along narrow yield lines as assumed in the yield line theory. In addition, the assumption of small deflections is shown to be invalid even at design loads obtained from the yield line theory. Experiments have shown that these large deflections lead to actual collapse loads two to four times larger than the yield line collapse loads. Thus, it is concluded that the yield line theory is not applicable for the analysis of this type of connection.

The main recommendation of this study is that, in cases where small deflections are essential, Blodgett's elastic method can be used to obtain design loads. However, if deflections are of minor concern, Kapp's yield line method can be utilized and leads to conservative values of design loads.

Finally, some suggestions are made for future research.

ACKNOWLEDGEMENTS

The author wishes to express sincere gratitude to his advisor, Dr. Subhash C. Anand, for his considerable input of time, energy and guidance, without which this work would not be a reality.

Appreciation is also expressed to the members of his graduate advisory committee, Drs. R. H. Brown and M. L. Morrell, for their critical review of the manuscript. Special thanks are given to the American Institute of Steel Construction and the Department of Civil Engineering for the financial assistance provided the author throughout the course of his studies.

Finally, the author wishes to acknowledge the love and support of his family and friends which have helped make the many long hours of hard work most rewarding.

TABLE OF CONTENTS

Table of Contents (Cont'd)

LIST OF TABLES

LIST OF FIGURES

List of Figures (Cont'd.)

CHAPTER I

PROBLEM DESCRIPTION

In the design of steel structures, light bracing of the type depicted in Figure 1.1 is frequently employed. When designing this type of tensile member, the usual procedure is to size the connection and assume the tension transfer. This approach, while appropriate for sizing the tension member and weld, neglects the strength of the web.

Blodgett (1) has suggested an elastic analysis procedure which takes into account the capability of the web in carrying the load. The method is straightforward, albeit, overly conservative. Abolitz and Warner (2) introduced the yield line concept for the analysis of these connections in 1965. Stockwell (3) later extended this theory to the analysis of welded beam-to-column connections. Shortly thereafter, the technique was refined further by Kapp (4) who, then, extended his refinements to the analysis of the bracing connection (5). In his work, bounding solutions of ultimate load are determined by first assuming the flange-web juncture to simulate a simple-support and then assuming full-fixity. It is shown through design examples that the web may not be adequate to carry the tensile load within the assumptions of the yield line theory (i.e., yielding occurs along narrow bands, deflections remain small and the material is elastic-perfectly plastic).

The lack of experimental data concerning the strength of this connection group prompted a pilot research program that was conducted at

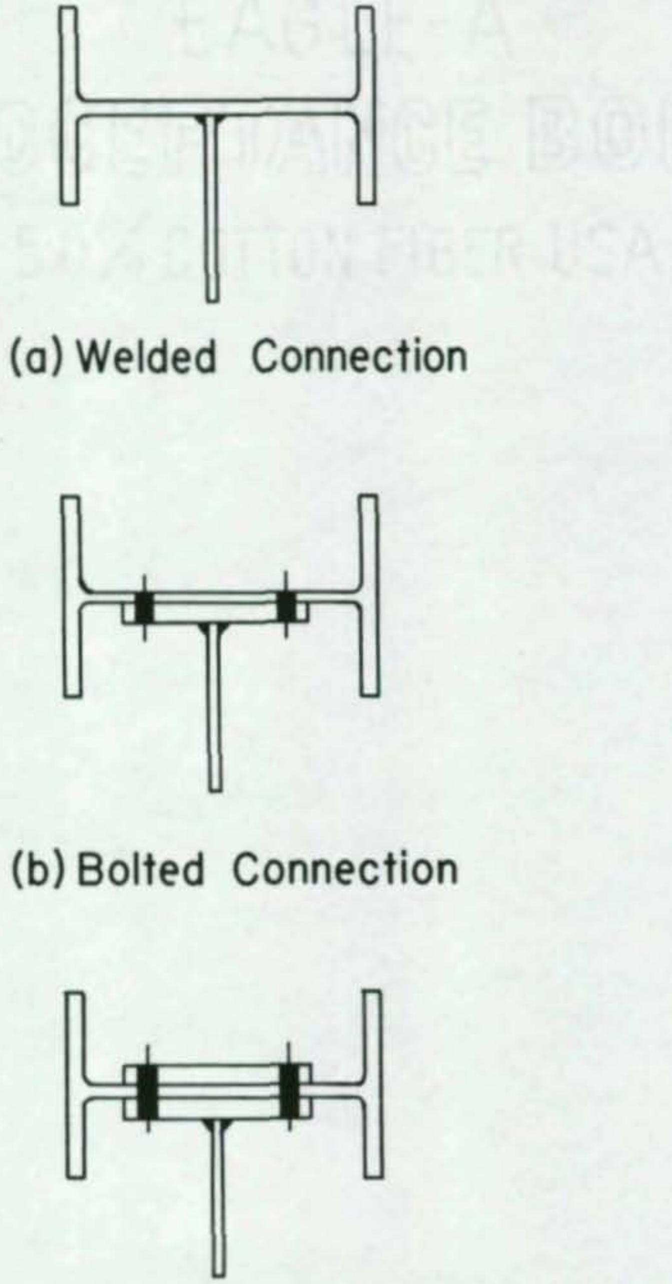

Figure 1.1. Typical Light Bracing Connections

Clemson University (6). Experimental tests indicated that the strength of these connections were, in general, much greater than predicted by the yield line theory. Moreover, the deflected shape of the web, when loaded in the post-elastic range, showed signs of yielding in broad bands rather than along narrow yield lines. Based upon these tests, it seems that the yield line theory may not be applicable to this class of problems. In fact, none of the previously cited techniques appear to accurately predict the development of the yield pattern or the load carrying capability of the connections in the plastic range.

In as much as the ultimate strength design is becoming an integral part of structural engineering, an in-depth understanding of connections designed for post-elastic strength capability becomes essential. As such, the motive and objective for this study is to shed further insight into the behavior of the aforementioned connection group in the plastic range by use of the finite element technique.

Details about the finite element model, along with the material elastic-plastic constitutive relations, yield criteria and solution method are presented in Chapter II. The elastic-plastic solutions for some typical connections are presented in Chapter III, with an evaluation of the data and current design practices given in Chapter IV. In Chapter V, conclusions with respect to the applicability of the yield line concept are made in addition to suggestions for further research in this area.

CHAPTER II

SOLUTION PROCEDURE

There are two possible approaches that can be taken when attempting to solve any structural problem. For most situations an exact solution is possible (in the form of tables or graphs). However, as the level of complexity increases, the ability to formulate and solve problems in an exact manner diminishes quickly. It is then that approximate (numerical) techniques must be employed. An elastic-plastic analysis generally falls into this category.

The two major tools available to the analyst are the 'finite difference' and 'finite element' methods. The former utilizes a technique whereby the governing partial differential equations are solved numerically. The later method, first introduced in the mid-1950's, involves partitioning a continuous system with infinite degrees of freedom into a finite number of subdivisions (or elements). The governing differential equations are solved exactly within each element. For each element, the stiffness is obtained by applying any one of a number of variational principles. Superposition of the individual stiffnesses forms the structural stiffness from which the solution for displacements, stresses and strains is readily found.

For this study the finite element technique is employed. The primary advantages are the relative ease of its application and the diverse nature of the problems which can be readily solved with it.

Displacement Method

The variational principle primarily used in finite element analysis is that of Minimum Potential Energy. The principle states that of all possible displacement states, the one to which the loaded structure will deform is that which yields the smallest value for the potential energy and satisfies the differential equations of equilibrium. The Minimum Potential Energy Principle is actually a statement of the principle of virtual work and shall be used as such in subsequent developments.

This approach is commonly referred to as the 'displacement' or 'stiffness' method. The method entails assuming a displacement function which uniquely describes the displacements within the element in terms of nodal point displacements. From geometric and material constitutive relations, stresses corresponding to the nodal displacements are determined. By application of the virtual work principle, nodal forces are derived which equilibrate the stresses distributed along the element boundaries. Carrying out these operations yields a relationship between nodal point forces and nodal point displacements. This relationship is defined by the stiffness matrix for the element.

The stiffness matrix for the total structure is obtained by a sytematic addition of the stiffness matrices of individual elements, and yields a set of equilibrium equations for the total structure relating nodal forces to nodal displacements. This assemblage renders only an approximation of the actual stiffness of the structure being modelled. However, for any finite element, there exist certain requirements which, when met, will generally guarantee convergence to exact solutions with decreasing element size. The mandatory criteria are

1. The displacement field within an element must be continuous (i.e., do not use terms such as $1/r$, $1/x$, etc.).

2. The displacement field must be able to model a state of constant strain (or curvature, in the case of plate bending).

3. Rigid body translation must be possible (i.e., include constant terms in the displacement function).

4. Compatibility of displacements (slopes) should generally exist between elements.

5. The element should have no preferred direction. This can be met by using 'complete' polynomials as displacement fields within an element.

Of the above criteria, all must be met except for requirement 4. It has been found that this condition for convergence is violated by many successful elements. This is believed to be a result of the satisfaction of requirement 2. In other words, elements satisfying requirement 2 also satisfy requirement 4 in the limit of mesh refinement as each element approaches a limit of constant strain (or curvature).

Further, incompatible elements (i.e., those not satisfying requirement 4) are often found to out-perform related compatible elements when working with meshes of practical size. This is due to the fact that discrete elements stiffen the system, whereas, non-compatibility of displacements makes the system more flexible. Each effect tends to cancel each other resulting in a model which closely approximates the true situation.

Elastic Stiffness of a Rectangular Element

The linear theory which will be employed throughout this development is commonly referred to as the small deformation theory of thin plate bending which assumes, in part

1. The plate is flat before and after deformation (i.e., curvatures $\ll 1$).

2. The plate thickness is small compared to its other dimensions.

3. The deflections are small compared to the plate thickness (on the order of one-third to one-half the plate thickness).

4. There is no straining of the middle surface of the plate.

5. Normals to the middle surface remain normal after deformations (transverse shearing is ignored).

With these limitations in mind, a relatively simple rectangular finite element can be developed for the elastic-plastic analysis of plate bending problems (Figure 2.1). This particular element was first proposed by Zienkiewicz and Cheung (7).

This element has three degrees of freedom per node that leads to a displacement function within the element which requires twelve constants. This displacement function can be given by

$$w = a_1 + a_2x + a_3y + a_4x^2 + a_5xy + a_6y^2 + a_7x^3 + a_8x^2y + a_9xy^2 + a_{10}y^3 + a_{11}x^3y + a_{12}xy^3. \tag{2.1}$$

Note that this is a complete cubic polynomial with the addition of two fourth-order terms to allow the inclusion of the last two coefficients a_{11} and a_{12}. These two terms maintain the non-directionality of the function so their inclusion is permissible (requirement 5 of the convergence criteria).

By using nodal values of slopes and displacements only in the development of this stiffness matrix, the displacement along any boundary of the rectangular element can be uniquely defined. However, this does not lead to identical normal slopes for two adjacent elements along a given boundary. Consequently, there is no inter-element compatibility of normal slope, and the displacement function chosen renders a non-compatible plate bending element. Nevertheless, it will

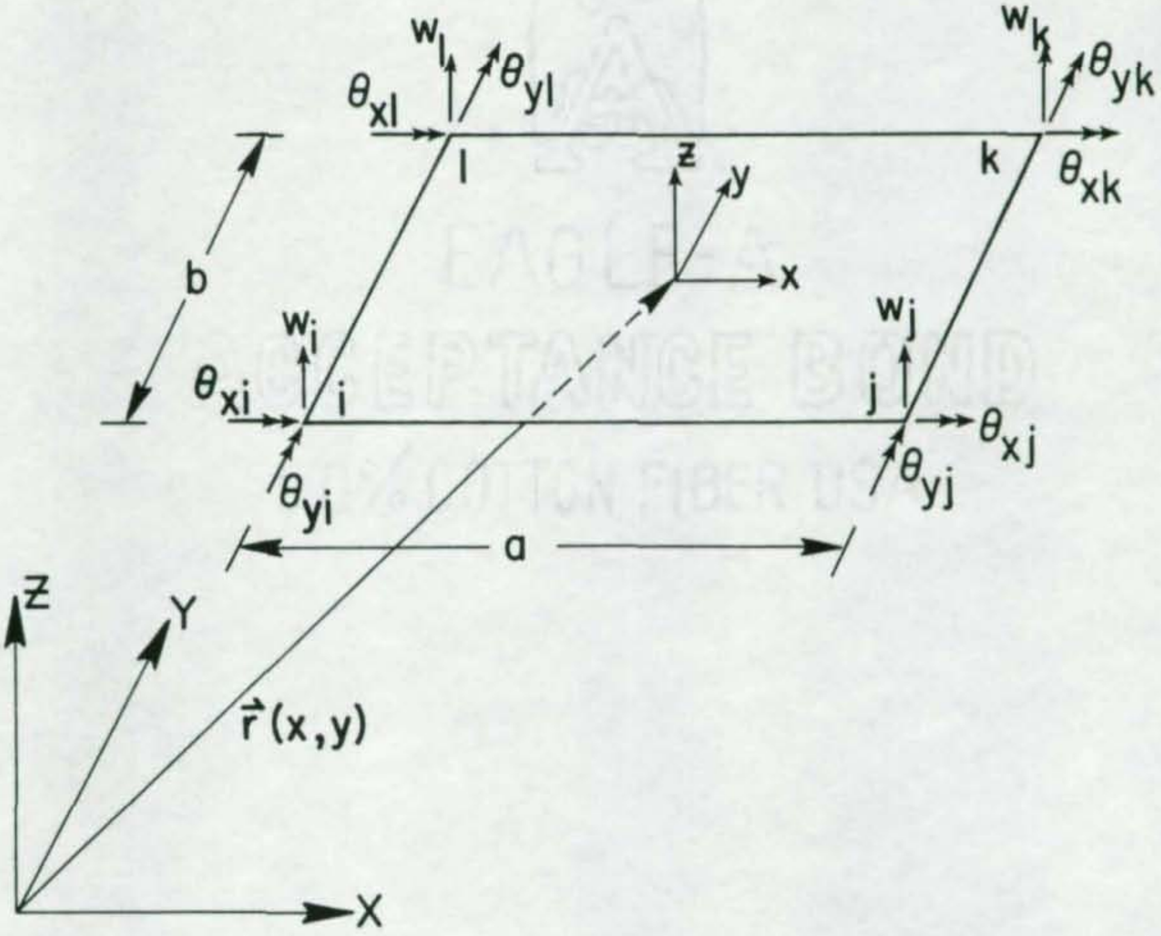

Figure 2.1. Sign Convention for Rectangular Plate Element

be shown later that the constant curvature criterion (requirement 2 of the convergence criteria) can be met by Equation (2.1) leading to the conclusion that convergence to a correct solution is assured.

The deflection vector for node i, for example, is given by

$$\{r_i\} = \begin{Bmatrix} w_i \\ \theta_{xi} \\ \theta_{yi} \end{Bmatrix} = \begin{Bmatrix} w_i \\ (\partial w/\partial y)_i \\ (-\partial w/\partial x)_i \end{Bmatrix} \quad . \tag{2.2}$$

Taking the indicated partial derivatives and specializing for each node results in the relationship

$$\{r\} = [C]\,\{a\} \quad , \tag{2.3}$$

where

$$[C] = \begin{bmatrix} 1 & x_i & y_i & x_i^2 & x_iy_i & y_i^2 & x_i^3 & x_i^2y_i & x_iy_i^2 & y_i^3 & x_i^3y_i & x_iy_i^3 \\ 0 & 0 & 1 & 0 & x_i & 2y_i & 0 & x_i^2 & 2x_iy_i & 3y_i^2 & x_i^3 & 3x_iy_i^2 \\ 0 & -1 & 0 & -2x_i & -y_i & 0 & -3x_i^2 & -2x_iy_i & -y_i^2 & 0 & -3x_i^2y_i & -y_i^3 \\ \multicolumn{12}{l}{\text{(same as for node i; permute subscripts i-j-k-l)}} \end{bmatrix} , \tag{2.4}$$

$$\{r\} = [r_i \; r_j \; r_k \; r_l]^T \quad , \tag{2.5}$$

$$\{a\} = [a_1 \; a_2 \; a_3 \; . \; . \; . \; a_{12}]^T \quad . \tag{2.6}$$

It should be pointed out that in order to facilitate integration, which will be required later, a local coordinate system is used throughout this formulation, in which the centroid of the rectangle is taken as the origin as shown in Figure 2.1. Solving Equation (2.3) for the displacement function coefficients results in

$$\{a\} = [C]^{-1}\,\{r\} \quad . \tag{2.7}$$

By geometric and material relationships, it can be shown that the moments and curvatures are related by

$$\{M\} = \begin{Bmatrix} M_x \\ M_y \\ M_{xy} \end{Bmatrix} = \frac{h^3}{12}[D]^e \begin{Bmatrix} -\partial^2 w/\partial x^2 \\ -\partial^2 w/\partial y^2 \\ 2\partial^2 w/\partial x \partial y \end{Bmatrix} = \frac{h^3}{12}[D]^e \{\kappa\} \quad , \tag{2.8}$$

where

$$[D]^e = \frac{E}{1-\nu^2} \begin{bmatrix} 1 & \nu & 0 \\ \nu & 1 & 0 \\ 0 & 0 & (1-\nu)/2 \end{bmatrix} ,$$

κ = curvature vector,

h = plate thickness.

The curvature vector is found by taking the indicated partial derivatives of Equation (2.1), which yields

$$\{\kappa\} = [Q]\ \{a\} = [Q]\ [C]^{-1}\ \{r\} \quad . \tag{2.9}$$

In Equation (2.9), [Q] is given by

$$[Q] = \left[[Q_o] \;\vert\; [Q_1] \;\vert\; [Q_2] \right] \quad , \tag{2.10}$$

in which

$[Q_o]$ = a (3x3) null matrix,

$$[Q_1] = \begin{bmatrix} -2 & 0 & 0 \\ 0 & 0 & -2 \\ 0 & 2 & 0 \end{bmatrix} \quad , \tag{2.11}$$

$$[Q_2] = \begin{bmatrix} -6_x & -2y & 0 & 0 & -6xy & 0 \\ 0 & 0 & -2x & -6y & 0 & -6xy \\ 0 & 4x & 4y & 0 & 6x^2 & 6y^2 \end{bmatrix} \quad . \tag{2.12}$$

From Equation (2.11), it is seen that the criterion for constant curvature is met (i.e., in the limit of mesh refinement, $[Q_2]$ tends to zero leaving only $[Q_1]$).

Applying the principle of virtual work, which states that the work performed by external nodal forces {F} acting through a virtual nodal displacement must equal the internal work of virtual deformations, leads to

$$[\delta r]^T \{F\} = \int_{area} [\delta\kappa]^T \{M\} \, dA \quad . \tag{2.13}$$

Using Equations (2.8) and (2.9), {M} can be expressed as

$$\{M\} = \frac{h^3}{12} [D]^e \{\kappa\} = \frac{h^3}{12} [D]^e [Q] [C]^{-1} \{r\} \quad , \tag{2.14}$$

and

$$[\delta\kappa]^T = [\delta r]^T [C]^{-1T} [Q]^T, \tag{2.15}$$

which upon substitution in Equation (2.13) leads to

$$\{F\} = \frac{h^3}{12} [C]^{-1T} \int_{area} [Q]^T [D]^e [Q] \, dA \, [C]^{-1} \quad . \tag{2.16}$$

Equation (2.16) is of the form

$$\{F\} = [k]^e \{r\} \quad ,$$

where

$$[k]^e = \frac{h^3}{12} [C]^{-1T} \int_{area} [Q]^T [D]^e [Q] \, dA \, [C]^{-1} \quad , \tag{2.17}$$

which is the elastic stiffness matrix for the rectangular plate bending element. An explicit expression for the integral has been derived and can be found in Appendix A.

Elastic-Plastic Constitutive Relationships

In this study, the material is assumed to be elastic-perfectly plastic. To ensure this, three aspects of the material behavior must be defined:

1. The elastic constitutive relations,
2. The criterion which will determine the transition from the elastic to plastic state,
3. The plastic constitutive relations.

Plate bending is a plane stress condition, for which one normal stress and two shearing stress components normal to the plane of the plate are negligible. Consequently, the stress-strain state can be given by the corresponding vectors

$$\{\sigma\} = \begin{Bmatrix} \sigma_x \\ \sigma_y \\ \sigma_{xy} \end{Bmatrix} , \tag{2.18}$$

and

$$\{\varepsilon\} = \begin{Bmatrix} \varepsilon_x \\ \varepsilon_y \\ 2\varepsilon_{xy} \end{Bmatrix} . \tag{2.19}$$

Elastic Constitutive Relations

For the elastic case, the well-known stress-strain relationship is

$$\{\sigma\} = \frac{E}{1-\nu^2} \begin{bmatrix} 1 & \nu & 0 \\ \nu & 1 & 0 \\ 0 & 0 & (1-\nu)/2 \end{bmatrix} \{\varepsilon\} = [D]^e \{\varepsilon\} , \tag{2.20}$$

for which the moment-curvature relationship is given by Equation (2.8).

Yield Criterion

The yield criterion is the condition which defines the limit of elasticity for a material under any combination of stresses in addition to its post-elastic behavior. The two yield criteria which are generally noted in the literature are those of von Mises and Tresca.

The Tresca yield criterion is based on the assumption that the maximum shearing stress governs yielding. A plot of the resulting yield locus in plane stress is a hexagon in the (x,y)-plane

(Figure 2.2). This criterion has primarily been found to apply in the study of non-ductile materials, such as cast iron.

The von Mises yield criterion is based on the premise that yielding begins when the elastic energy of distortion (shearing) reaches a critical value. As a result, it can be seen that hydrostatic stress states have no effect on the commencement of yielding (8). For most ductile materials acted on by moderate hydrostatic stresses, this will be found to be fairly accurate. As such, experiments have shown that the von Mises yield criterion holds reasonably well for ductile materials but overestimates the initiation of yielding in a non-ductile material. For this study, A36 steel (a ductile material) is used and, as such, the von Mises criterion shall be assumed in the plastic state.

The von Mises yield criterior can be written for a two-dimensional stress state as

$$\sigma_1^2 - \sigma_1 \sigma_2 + \sigma_2^2 = \sigma_o^2 \quad , \tag{2.21}$$

or

$$\sigma_x{}^2 - \sigma_x\sigma_y + \sigma_y{}^2 + 3\sigma_{xy}{}^2 = \sigma_o^2 \tag{2.22}$$

where σ_o = the yield stress of the material in simple tension, and σ_1 and σ_2 are principal stress components. A plot of Equation (2.21) is seen to be an ellipse which encloses the yield loci of the Tresca criterion as shown in Figure 2.2.

Plastic Constitutive Relations

Plastic flow takes place once the stresses reach the yield surface. This plastic flow is generally taken to be governed by the Prandtl-Reuss theory (8, 9) which states that the rate of change of the plastic

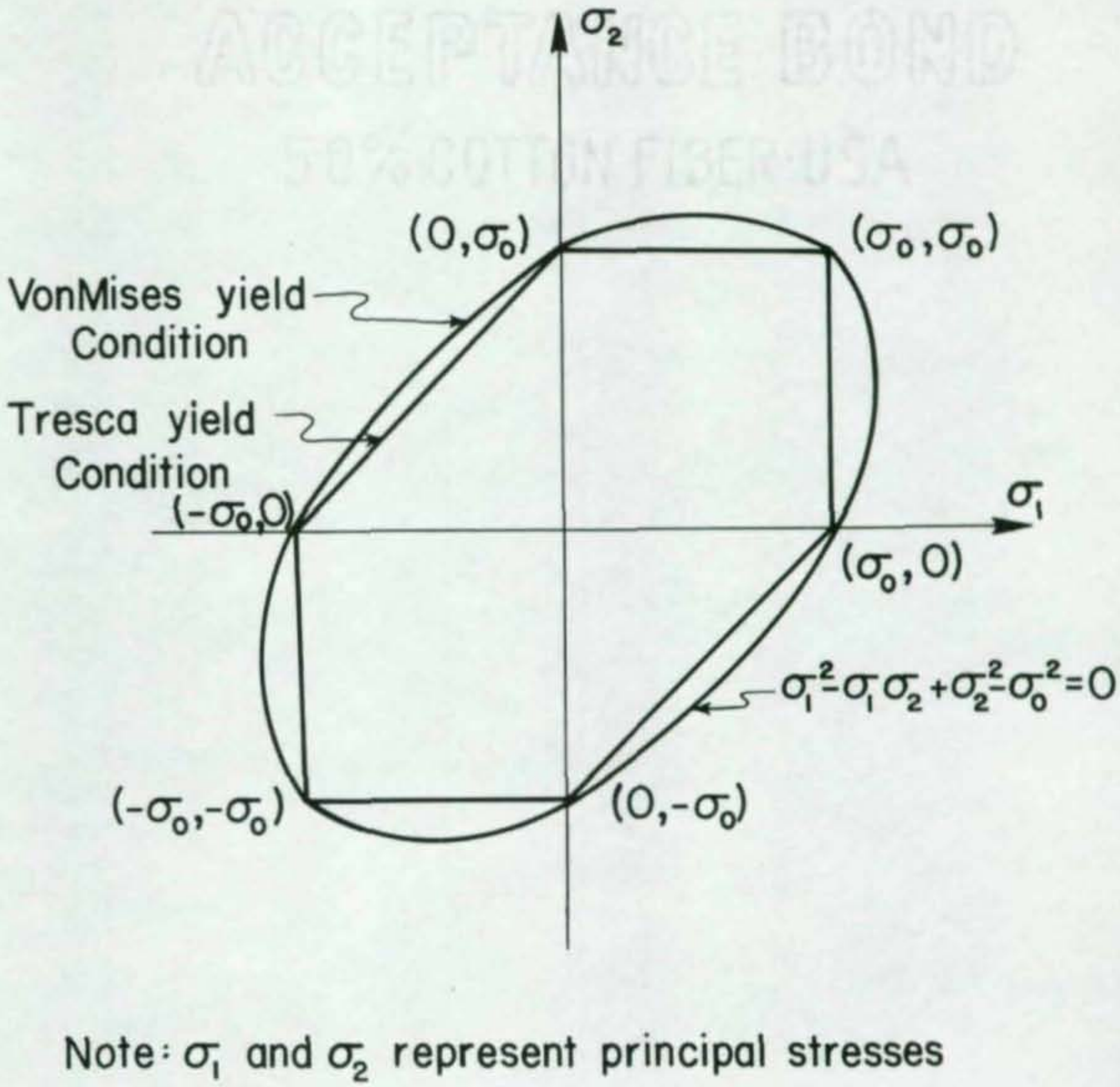

Figure 2.2. Tresca and von Mises Yield Criteria in Plane Stress

strain $d\varepsilon^p_{ij}$, at any instant, is proportional to the instaneous stress deviation σ'_{ij}.* This can be expressed mathematically as

$$d\varepsilon^p_{ij} = \sigma'_{ij}\ d\lambda \quad , \tag{2.23}$$

in which $d\lambda$ is a non-negative constant of proportionality.

Yamada (11) has developed an explicit expression for a plastic stress-strain matrix which is derived by inverting the Prandtl-Reuss equations in plasticity theory. The matrix is simple, straightforward and facilitates the incremental treatment of elastic-plastic problems. Assuming a non-strain hardening material, this matrix is given by

$$[D]^p = \frac{E}{\zeta} \begin{bmatrix} s_y^2 + 2\eta & -s_x s_y + 2\nu\eta & -\frac{\sigma_{xy}}{1+\nu}(s_x + \nu s_y) \\ & s_x^2 + 2\eta & -\frac{\sigma_{xy}}{1+\nu}(s_y + \nu s_x) \\ \text{SYM.} & & \xi/[2(1+\nu)] \end{bmatrix} , \tag{2.24}$$

where

$$\eta = \sigma^2_{xy/(1+\nu)},$$

$$\xi = s_x^2 + 2\ s_x s_y + s_y^2 \quad ,$$

and

$$\zeta = \xi + 2(1 - \nu^2)\eta \ ,$$

$$s_x = \frac{1}{3}\ (2\sigma_x - \sigma_y) \quad ,$$

$$s_y = \frac{1}{3}\ (2\sigma_y - \sigma_x) \quad .$$

---

*Dubey (10) has proposed a new incremental flow theory which is a modification of this classical flow theory. His concept shows promise but has yet to be verified.

Sandwich Plate vs. Elasto-Plastic Plate Element

In the literature there are primarily two lines of thought concerning the elastic-to-plastic phase of the plate analysis problem. Some researchers (12, 13) have utilized a simplified model commonly referred to as a 'sandwich' plate model, which is shown in Figure 2.3 along with the sign convention for moments used in this study. It is composed of a core material, which carries all of the transverse shear, sandwiched between two thin cover plates, which support only membrane stresses, whose middle surfaces are separated by the real plate thickness, h. For the purely elastic situation, an exact equivalency is possible with the homogeneous thin plate if the cover plate thickness is taken as one-sixth the thickness of the true plate.

The sandwich plate arrangement simplifies the inelastic analysis considerably. The cover sheets are composed of an elastic-perfectly plastic material that obeys the yield conditions and the plastic flow criteria presented in the previous section. In the completely plastic state, equivalency of an homogeneous plate to a sandwich plate can be established by taking the thickness of each cover plate to be equal to one-fourth the thickness of the real plate. As such, the plate element is taken to be either completely elastic or completely plastic with no provision made for a transition from one state to the other.

A preliminary study conducted with this type of formulation produced ultimate loads that were much smaller than those predicted by Kapp's yield line theory (5) which gives an upper-bound solution. While the development of the yield patterns were as expected, it was found that the sandwich model is too flexible and that a transition of some form is required.

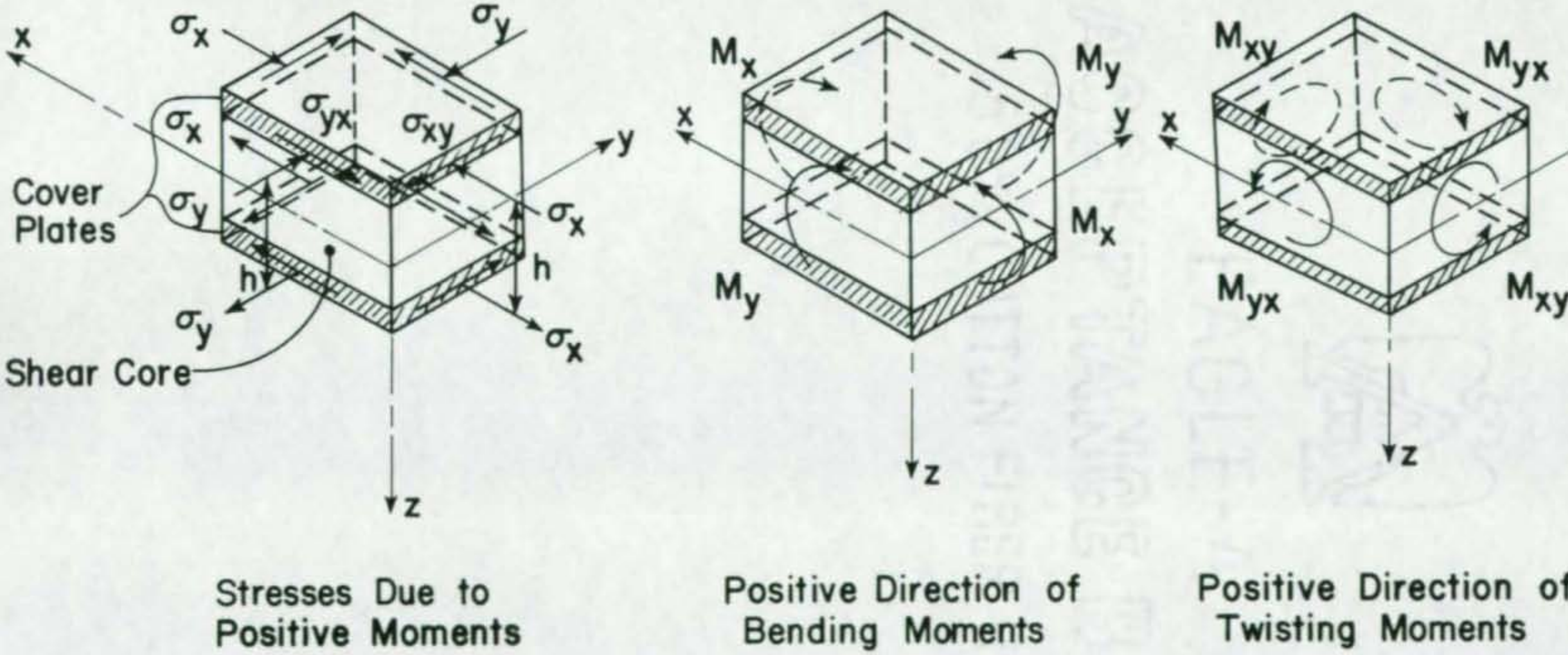

Figure 2.3. Sandwich Plate Configuration

Other researchers (14, 15) have applied a more exact technique of layering the plate into a discrete number of plane stress elements. The elastic-plastic state of each layer is determined and numerical integration is carried out to form the stiffness of the super element. This method, although quite accurate, is nonetheless prohibitive in terms of computer storage and execution time requirements. As such, another approach which incorporates the simplicity of the sandwich model and much of the accuracy of the layered-element model has been developed in this study.

The basic concept of the new model is that the plate element, after it reaches the plastic state, is divided into two regions. The outermost regions are represented as plastic fibers and the inner region is composed of the remaining elastic fibers through the plate thickness. The determination of the bending stiffness for the elasto-plastic plate element is explained in the following section.

Plastic Zone Extent Factor

For the small deformation theory being used in this study, the assumption is made that plane sections remain plane after deformation. A direct consequence is that all strains vary linearly along the depth of the plate.

Within the elastic region of the partially plastic section, stresses reach a level such that the von Mises yield condition is just satisfied. All fibers located at a depth greater than this 'initial yield' depth are already plastic. If one defines the equivalent stress as

$$\sigma_x^2 - \sigma_x \sigma_y + \sigma_y + 3\sigma_{xy}^2 = \sigma_{eq}^2 \quad , \tag{2.25}$$

then, σ_{eq} is equal to the yield stress σ_o in the plastic portion and less than σ_o in the elastic portion of the plate cross-section.

The stresses within the elastic portion of the cross-section may be related to the strain by the well-known elastic stress-strain relationships and are given by

$$\begin{aligned} \sigma_x &= D^* (\varepsilon_x + \nu\varepsilon_y) \quad , \\ \sigma_y &= D^* (\varepsilon_y + \nu\varepsilon_x) \quad , \\ \sigma_{xy} &= D^* (1 - \nu)\, \varepsilon_{xy} \quad , \end{aligned} \tag{2.26}$$

where

$$D^* = E/(1 - \nu^2) \quad .$$

Substituting Equation (2.26) into Equation (2.25) gives

$$\begin{aligned} D^{*2} \; [(\varepsilon_x+\nu\varepsilon_y)^2 - (\varepsilon_x+\nu\varepsilon_y)(\nu\varepsilon_x+\varepsilon_y) + (\nu\varepsilon_x+\varepsilon_y)^2 \\ + 3\,\{(1-\nu)\,\varepsilon_{xy}\}^2] = \sigma_{eq}^2 \quad , \end{aligned} \tag{2.27}$$

in which σ_{eq} is less than or equal to σ_o.

Expanding and collecting terms leads to

$$(1-\nu+\nu^2)(\varepsilon_x^2+\varepsilon_y^2) - (1-4\nu+\nu^2)\,\varepsilon_x\varepsilon_y + 3\,\{(1-\nu)\,\varepsilon_{xy}\}^2 = \varepsilon_{eq}^2 \tag{2.28}$$

in which ε_{eq} = reduced strain = σ_{eq}/D^*.

From the von Mises yield criterion it is required that at the initial yield fiber depth, σ_{eq} be equal to σ_o. Therefore,

$$\varepsilon_{eq} = \frac{\sigma_{eq}}{D^*} = \frac{\sigma_o}{D^*} = \varepsilon_o \quad , \tag{2.29}$$

in which ε_o = reduced strain at the initial yield fiber depth. Therefore, the depth of yielding at any load level can be determined by equating the expression of the reduced strain given by Equation (2.28) to ε_o. It now remains to relate this information in such a way that the extent of the plastic zone in the cross-section can be determined.

From the linearity of the strain variation, the strain at any depth, d, can be related to that of the outer fibers by

$$\varepsilon_{ij}^{d} = \frac{2d}{h}\,\varepsilon_{ij}^{h} \quad , \tag{2.30}$$

where ε_{ij}^{h} and ε_{ij}^{d} are the strains at depth h and d, respectively.

From Equation (2.28), it can be seen that the reduced strain also varies linearly. Therefore, Equation (2.30) can be rewritten in terms of the reduced strain as

$$\varepsilon_{eq}^{d} = \frac{2d}{h}\,\varepsilon_{eq}^{h} \quad . \tag{2.31}$$

Although the reduced strain, as given by Equation (2.28), is valid only in the elastic region of the plate thickness, this expression may be utilized for determining ε_{eq}^{h}. The reduced strain at the outer fibers of the plate thickness is required in order to find the location for which ε_{eq}^{d} is equal to ε_o. From Equation (2.31), this relationship is seen to be

$$\frac{\varepsilon_o}{\varepsilon_{eq}^{h}} = \frac{2d}{h} \quad . \tag{2.32}$$

Rearranging and letting $\phi = \frac{d}{h}$, yields the plastic zone extent factor, ϕ, as

$$\phi = \frac{1}{2}\,\frac{\varepsilon_o}{\varepsilon_{eq}^{h}} \quad . \tag{2.33}$$

Stiffness of Elasto-Plastic Element

In order to find the incremental stiffness relationship for the partially plastic plate element, the incremental moment-curvature relationships are needed. The generalized incremental relation is given by

$$\{\Delta M\} = \int_{-h/2}^{h/2} [D]\ \{\Delta\kappa\} z^2 dz \quad , \tag{2.34}$$

in which $\{\Delta M\}$ and $\{\Delta\kappa\}$ are the incremental moment and curvature vectors given in Equation (2.8) and [D] is the generalized incremental moment-curvature matrix in the plastic range. The matrix [D] can be expanded into elastic and plastic parts as $[D]^e$ and $[D]^p$ which are defined in Equations (2.20) and (2.24), respectively.

Within the plastic region, the equivalent stress remains uniform for the perfectly plastic material, so the moments depend not on a variation of z but rather on ϕ (refer to Figure 2.4). The contribution to the incremental moments from the plastic zone, using strains at the mid-depth of the plastic region as an approximation of the strains throughout the plastic region, can be given by

$$\{\Delta M\}^p = 2\ (\tfrac{1}{2} - \phi)\ h\frac{h^2}{2}\ (\tfrac{1}{2} + \phi)^2\ [D]^p\ \{\Delta\kappa\} \quad . \tag{2.35}$$

Upon simplification, Equation (2.35) yields

$$\{\Delta M\}^p = (\tfrac{1}{8} + \tfrac{\phi}{4} - \tfrac{\phi^2}{2} - \phi^3)\ h^3\ [D]^p\ \{\Delta\kappa\} \quad . \tag{2.36}$$

The corresponding moment contribution of the elastic part of the section is given by

$$\{M\}^e = \tfrac{2}{3}\ \phi^3 h^3\ [D]^e\ \{\Delta\kappa\} \ . \tag{2.37}$$

The total incremental moment is, then, the sum of Equations (2.36) and (2.37).

The incremental stiffness matrix for the elasto-plastic element may be determined in a straightforward manner by simply using these

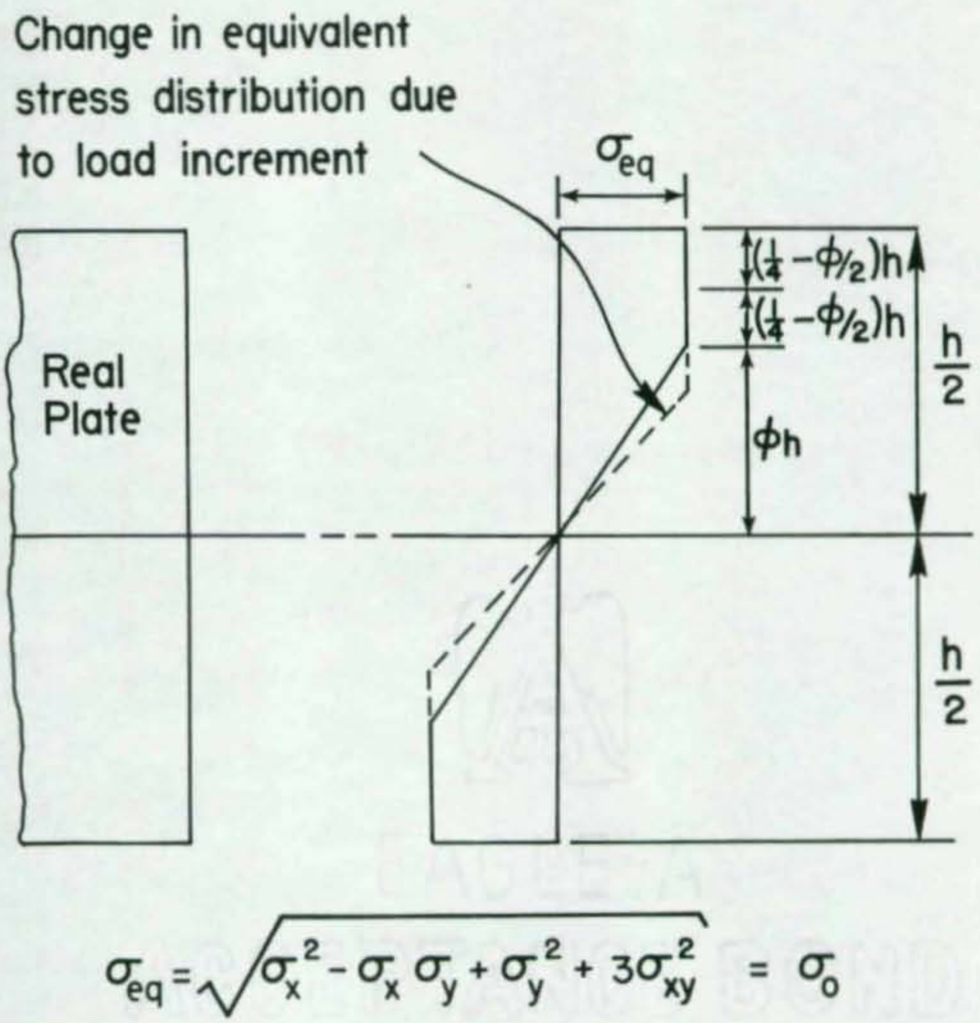

Figure 2.4. Equivalent Stress Distribution in Elasto-Plastic Element

incremental moment-curvature relations in conjunction with Equation (2.17). For the plastic part of the element stiffness matrix, the incremental plastic constitutive matrix $[D]^p$ is substituted for $[D]^e$ and the rigidity term $h^3/12$ replaced by

$$\left(\frac{1}{8} + \frac{\phi}{4} - \frac{\phi^2}{2} - \phi^3\right) h^3 \tag{2.38}$$

in Equation (2.17).* The elastic portion of the incremental stiffness is determined by using the elastic constitutive matrix $[D]^e$ as given in Equation (2.20) and replacing the rigidity term in Equation (2.17) with

$$\frac{2}{3} \phi^3 h^3 \quad . \tag{2.39}$$

The total incremental stiffness matrix is then found by superposition of the individual stiffness matrices representing the plastic and elastic contributions.

As can be readily surmised, this development assumes that the stresses are the same throughout the depth of the plastic zone. This is not strictly true. It is obvious that this apparent discrepancy can be minimized by dividing the plastic zone into a series of layers, each of which is treated individually as a plane stress case. This method would require a large increase in computer storage and execution time. This is, of course, undesirable. However, by limiting the magnitude of the deflections and corresponding strains within the small deformation range, the extent of the plastic zone is not developed enough to allow for significant stress variation. The difference

---

*Due to the variability of $[D]^p$ and ϕ, total stresses and strains obtained after a previous load increment are used to evaluate these quantities for the succeeding load increment.

between the assumed and real stress distribution can, therefore, be disregarded.

Method of Analysis

The non-linear analysis procedure utilizes a piecewise linear incremental technique which uses the Newton-Raphson iteration scheme to ensure that the correct load-deflection path is followed.

As the elastic part of the solution is linear, a load can be applied to the plate which will bring some element(s) in the mesh just to the point of initial yield, as determined from Equation (2.22). The load which will result in this first yield can be determined as follows. Apply an arbitrary load, P, that results in the moments M_x, M_y and M_{xy}. For a linear-elastic material, a factored load βP will result in the factored moments βM_x, βM_y and βM_{xy}.

The von Mises yield condition given by Equation (2.22) may be expressed as

$$M_x^2 - M_x M_y + M_y^2 + 3M_{xy}^2 = M_o^2 \quad , \qquad (2.40)$$

in which $M_o = \sigma_o h^2/6$. The load for which the yield condition is satisfied is, thus, given by

$$\beta^2 \, [M_x^2 - M_x M_y + M_y^2 + 3M_{xy}^2] = M_o^2 \quad . \qquad (2.41)$$

in which β is the scaling factor. This is a quadratic equation in β, the solution for which is given by

$$\beta = \frac{\pm M_o}{\sqrt{M_x^2 - M_x M_y + M_y^2 + 3M_{xy}^2}} \quad . \qquad (2.42)$$

The smallest positive value of the scaling factor for all the elements in the mesh is used to modify the original arbitrary load, P, to obtain the first yield load for the entire system of elements.

Once the load which initiates yielding in the plate has been found, the incremental load which will cause yielding in the next elastic element is determined. Again, an arbitrary incremental load, ΔP, is applied resulting in the corresponding incremental moments ΔM_x, ΔM_y and ΔM_{xy}. Note that in applying ΔP, all incremental stiffness matrices for plastic elements must be derived using Equations (2.36) and (2.37), and used in the total stiffness matrix. Assuming linearity of incremental load-deflection behavior within the load increment, factoring the load by β will result in the factored incremental moments $\beta \Delta M_x$, $\beta \Delta M_y$ and $\beta \Delta M_{xy}$.

The von Mises yield condition must be satisfied for an elastic element to become plastic which requires that

$$(M_x + \beta \Delta M_x)^2 - (M_x + \beta \Delta M_x)(M_y + \beta \Delta M_y) + (M_y + \beta \Delta M_y)^2 + 3(M_{xy} + \beta \Delta M_{xy})^2 = M_o^2 \quad , \tag{2.43}$$

for each elastic element. Note that in Equation (2.43), M_x, M_y and M_{xy} are the total moments at the end of the previous load increment. Equation (2.43) can be expanded into the quadratic form

$$(\Delta M_x^2 - \Delta M_x \Delta M_y + \Delta M_y^2 + 3\Delta M_{xy}^2)\beta^2 + [\Delta M_x (2M_x - M_y) + \Delta M_y (2M_y - M_x) + 6\Delta M_{xy} M_{xy}]\beta + (M_x^2 - M_x M_y + M_y^2 + 3M_{xy}^2 - M_o^2) = 0 \quad , \tag{2.44}$$

which is of the form: $a\beta^2 + b\beta + c = 0$. The solution of this quadratic equation is given by

$$\beta = \frac{-b \pm \sqrt{b^2 - 4ac}}{2a} \quad , \tag{2.45}$$

where

$$a = \Delta M_x^2 - \Delta M_x \Delta M_y + \Delta M_y^2 + 3\Delta M_{xy}^2 \quad ,$$

$$b = \Delta M_x (2M_x - M_y) + \Delta M_y (2M_y - M_x) + 6\Delta M_{xy} M_{xy} \quad ,$$

$$c = M_x^2 - M_xM_y + M_y^2 + 3M_{xy}^2 - M_o{}^2 \quad .$$

The smaller positive real root of Equation (2.45) is the scaling factor to be applied to ΔP in order for the elastic element to become plastic in any given load increment. By finding the smallest value of all the scaling factors, the load increment for which a previously elastic element will just reach the yield point can be determined.

Once this load increment has been determined and applied, it might be found that elements which are already plastic may violate the yield criterion upon addition of the incremental stresses to the existing total stresses. This exceedance must be corrected. It is for this occurrence that the Newton-Raphson iteration technique is employed. The procedure is outlined in Appendix B.

By successively applying incremental loads which initiate yielding in elastic elements, the sequential yielding of elements can be correctly traced. Application of the Newton-Raphson method ensures that the yield condition is satisfied by the stresses in the plastic elements, thus, guaranteeing a correct load-deflection path within the inelastic range.

Stability of Solution

Under a monotonically increasing load, unloading of plastic regions does not occur unless the plasticity develops to such an extent that the principal stress and plastic-strain increment axes reverse orientation, in which case, the plastic work (or more specifically, the work of distortion) becomes negative. This work can be expressed as (8)

$$dW_p = \sigma'_{ij}\, d\varepsilon^p_{ij} = \frac{2}{3}\sigma_o^2 \;\; d\lambda \quad , \tag{2.46}$$

where

$$d\lambda = \frac{3}{2\sigma_o^2\,(1-\nu)}\Big[(s_x+\nu s_y)\; d\varepsilon_x + (s_y+\nu s_x)\; d\varepsilon_y$$

$$+ 2\,(1-\nu)\;\sigma_{xy}\; d\varepsilon_{xy}\Big] \quad . \qquad (2.47)$$

The terms in Equation (2.47) have been previously defined.

Ordinarily, when the plastic work becomes negative, the plastic element becomes elastic again until such time as Equation (2.46) becomes positive and the yield criterion is satisfied. However, for a monotonically increasing load, the initiation of unloading is indicative of the plastic region expanding to such an extent that large plastic strains are possible without significant increase in load (i.e., instability). For a non-hardening material, this is visualized as representing the collapse load which would be obtained by limit analysis. This instability can be of a global or local nature. In regions of high stress concentration, it is possible for local instability to arise. As indicated in the work of Marcal (16), when Equation (2.46) becomes negative, program execution is halted rather than returning the unloading plastic element to the elastic state. Indication of unloading by a negative value of $d\lambda$ in Equation (2.47), as experienced in the examples presented in Chapter III, shows that failure is imminent and further increase in load is not possible. The plastic regions simply extend very rapidly under an insignificant increase in load.

CHAPTER III

RESULTS OF THE FINITE ELEMENT ANALYSIS

Description of the Computer Model

In order that the available experimental data (6) can be utilized for a meaningful evaluation of the mathematical model described in Chapter II, a connection system consisting of a W10x21 wide-flange section of three-foot length with 4"x3/8" and 8"x3/8" tension plates is used for the computer analysis as shown in Figure 3.1.

Due to symmetry, only one-fourth of the connection need be modelled. After some preliminary analyses were performed to determine the necessary element configurations, the meshes shown in Figures 3.2 (a) and (b) were selected, which are composed of 210 rectangular plate bending elements interconnected by 242 nodes with three degrees of freedom per node.

To simulate the effect of the tension plate width and fillet weld (taken to be three-eights of an inch on edge), an effective width of one-half inch, over which no rotation of the underlying web elements occurs, is assumed in the model. The load is assumed to be distributed uniformly to each of the nodal points located under the tension plate.

The plate bending model, as developed in the previous chapter, is capable of only planar analyses. A method whereby the out-of-plane flanges of a W10x21 section can be modelled in this analysis is necessary. Experimental evidence (6) has shown that, as the load is applied to the tension plate and the web deflects, the flanges remain plane and simply rotate in a rigid body motion. This indicates that plasticity

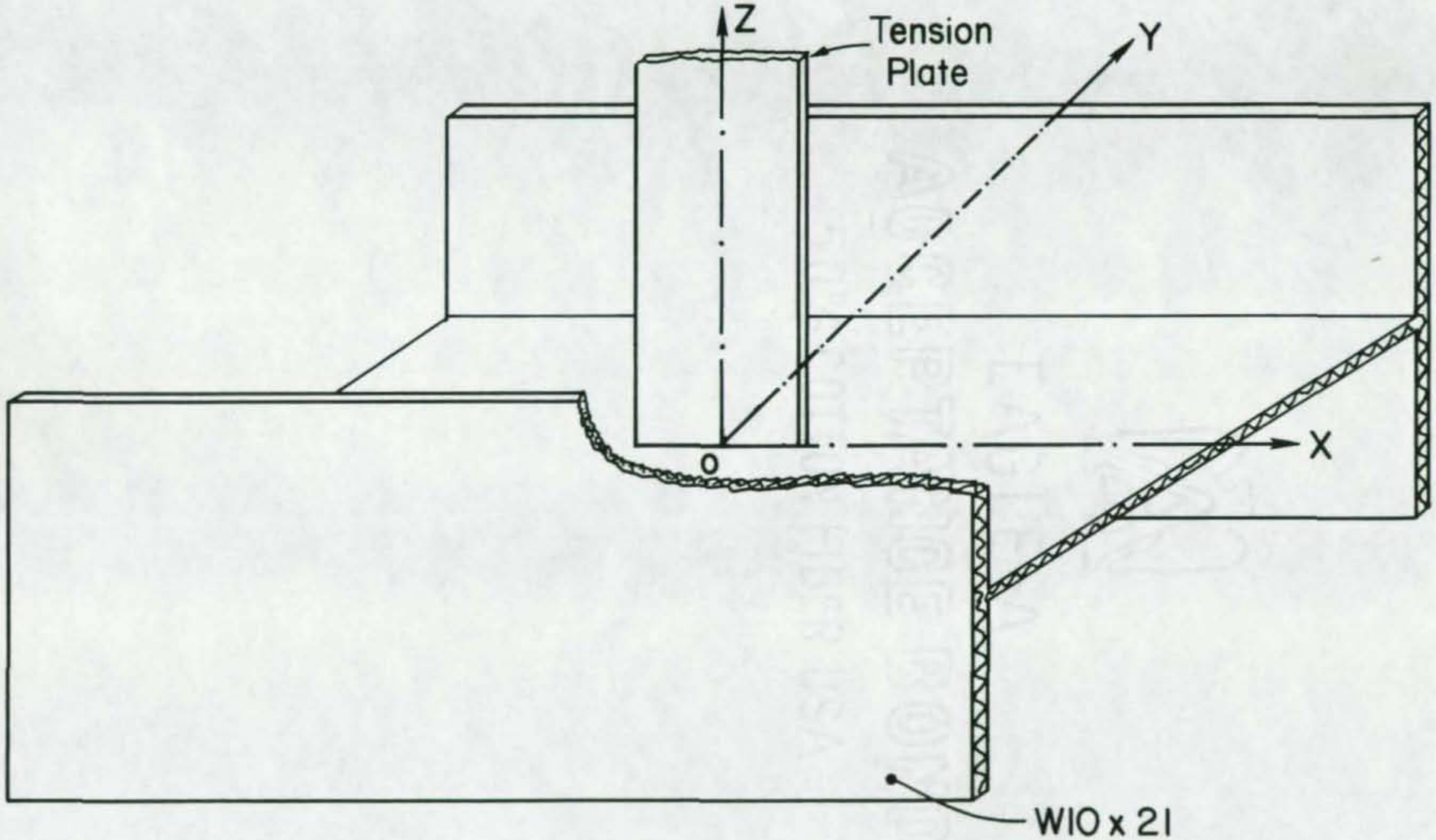

Figure 3.1. Light Bracing Connection Used in Analysis

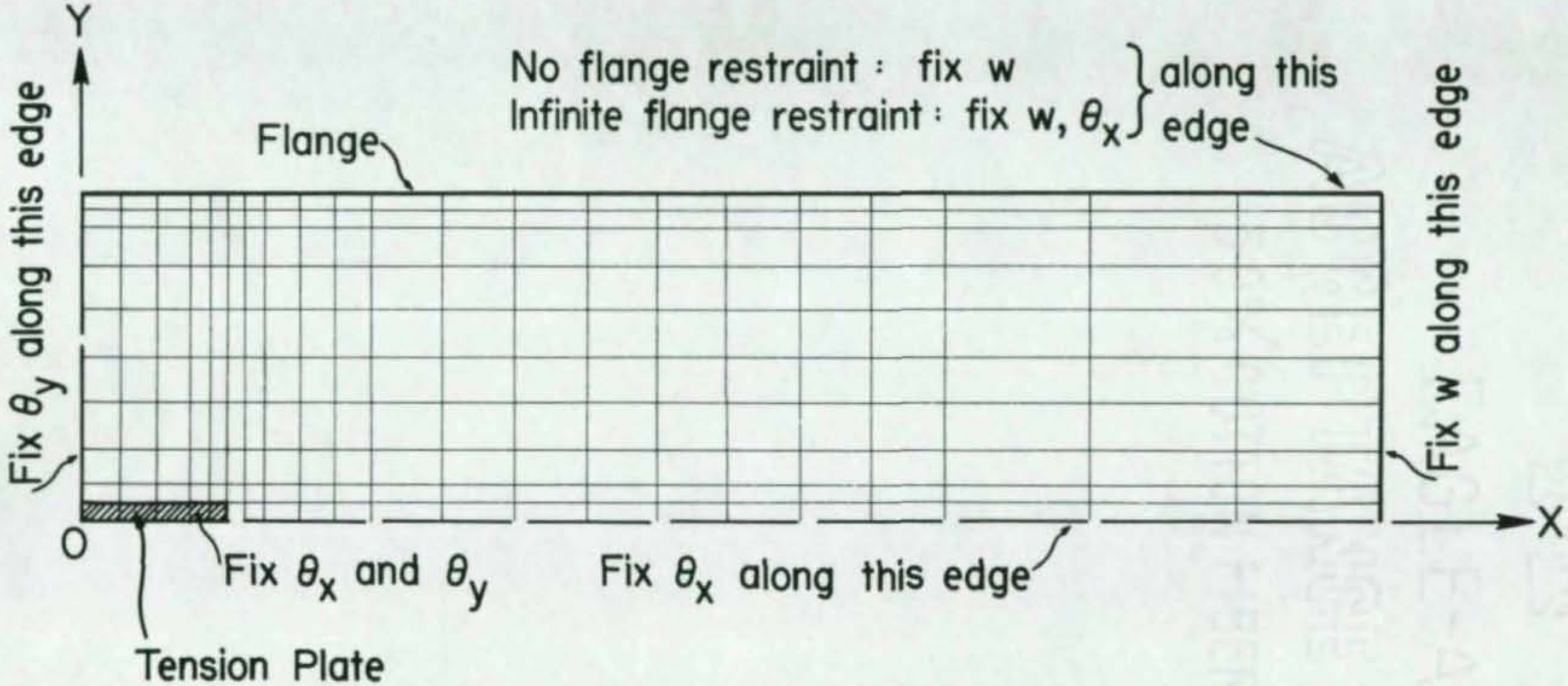

(a) 4" Tension Plate Mesh Pattern

Figure 3.2. Mesh Patterns and Boundary Conditions Used in Finite Element Analysis

Figure 3.2 (Cont'd.)

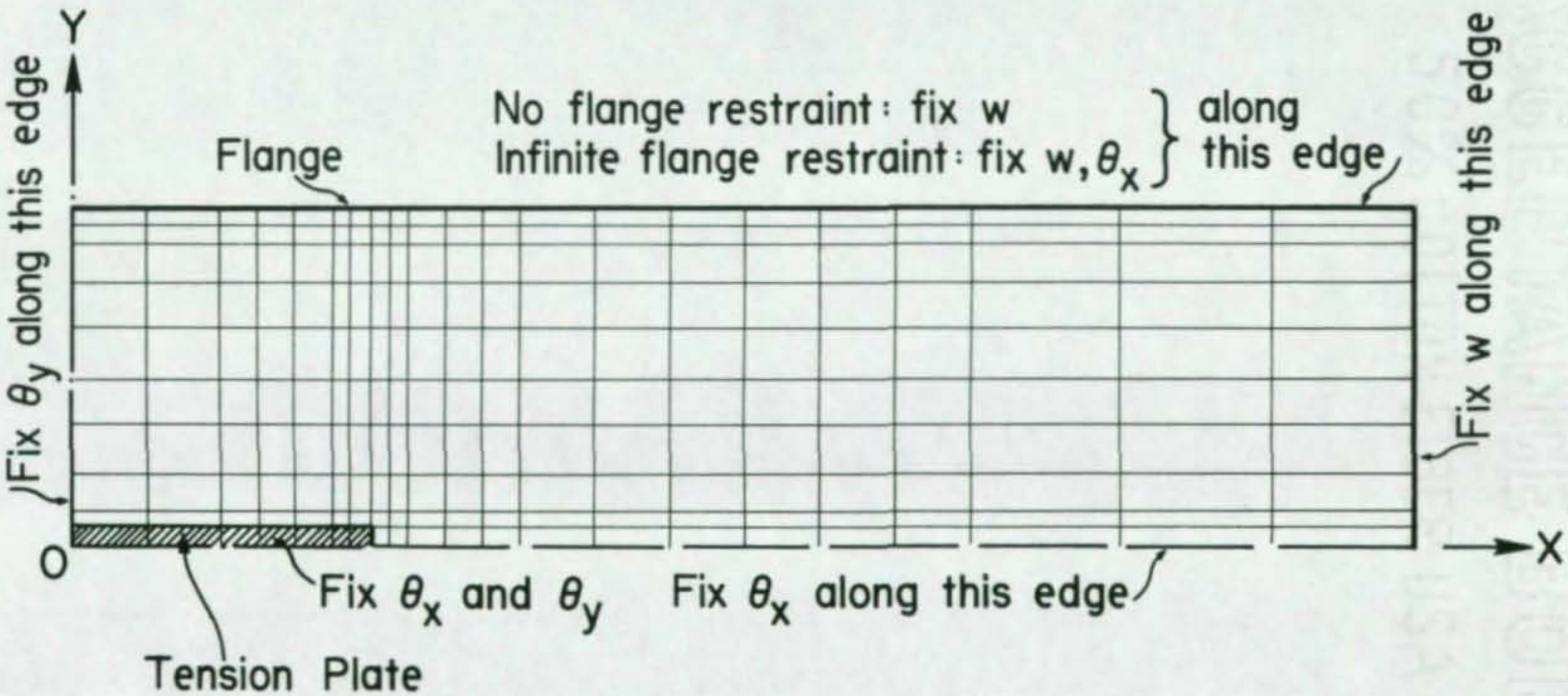

(b) 8" Tension Plate Mesh Pattern

is of minor concern in the flanges and that any flange model need only simulate the flanges in an elastic manner. As such, a simple flange model consisting of a two-node beam element with torsional capability having one displacement and two rotational degrees of freedom per node (the same as for the plate element) is proposed. This element is widely used and the details of the stiffness formulation are shown in Appendix E.

An elastic analysis using a W10x21 section and a four inch wide tension plate was performed. A comparison made with experimental strain gage data at a load of one thousand pounds, as shown in Figure 3.3, indicates a very close agreement between the measured and calculated strains in the elastic range, thereby, assuring the accuracy of the proposed finite element model.

Sandwich vs. Elasto-Plastic Formulation

A comparison of the sandwich plate and more exact elasto-plastic plate models indicates that the development of the yield patterns is essentially the same for both models. However, the collapse load for the elasto-plastic plate model is significantly higher (on the order of 25-30%). Table 3.1 gives a listing of the ultimate loads as determined by the computer analyses using the sandwich and elasto-plastic models.

A more apparent difference between the two computer models can be seen in Figure 3.4 in which the deflection curve for the sandwich model flattens out very rapidly after plasticity begins to develop. The curve for the elasto-plastic model shows a much more gradual flattening. A slower degradation of the bending stiffness is indicative of the inherent strength of the remaining elastic portion of the

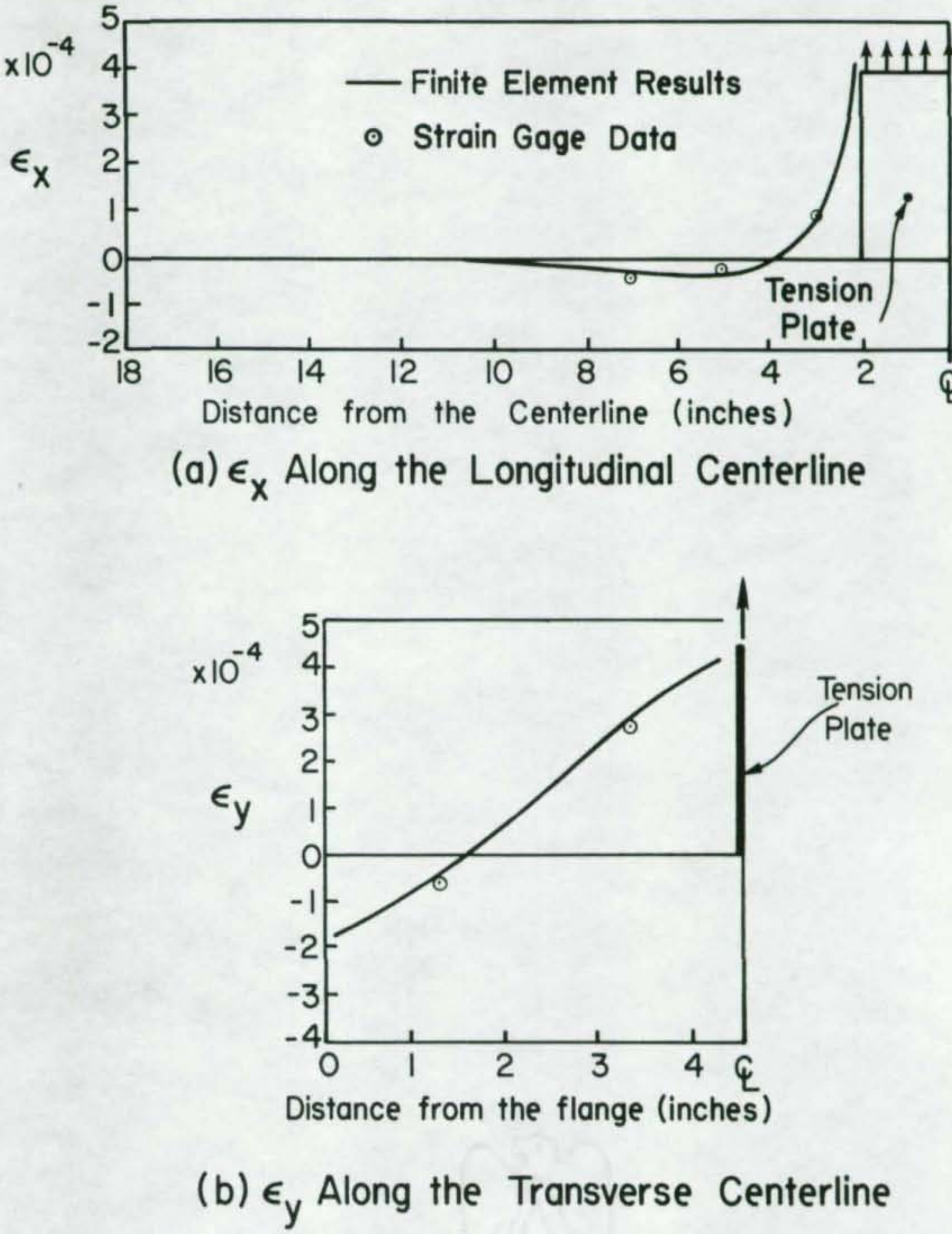

Figure 3.3. Comparison of Analytical and Experimental Strains with 4" Tension Plate

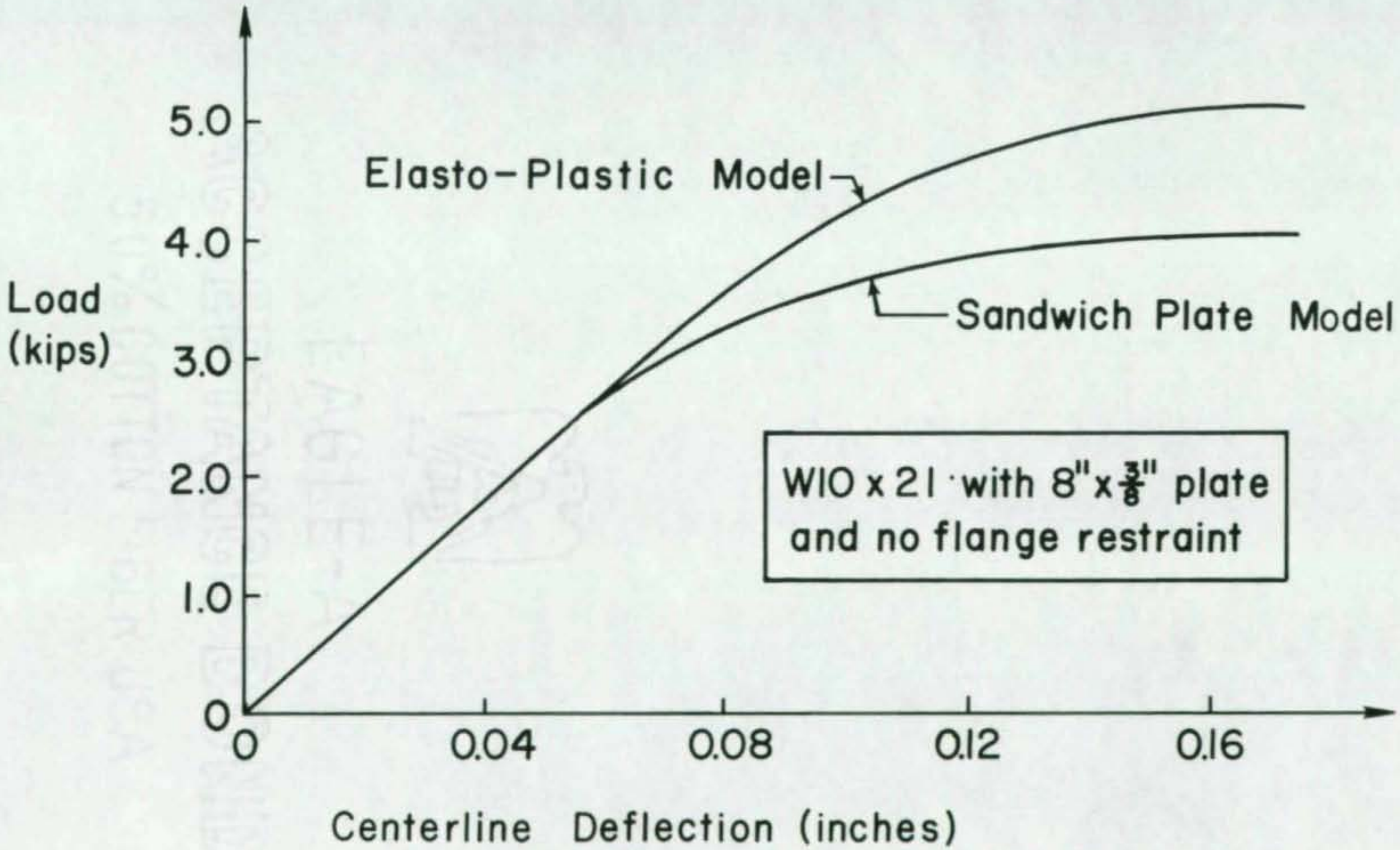

Figure 3.4. Stiffness Comparison of Sandwich and Elasto-Plastic Plate Models

Table 3.1. Ultimate Loads Using Sandwich and Elasto-Plastic Models

Member	Tension Plate	Flange Restraint	Ultimate Load (kips)	
			Sandwich Model	Elasto-Plastic Model
W10x21	4"	None	3.1	4.1
"	"	Simulation	4.4	5.4
"	"	Infinite	5.5	7.0
"	8"	None	4.1	5.0
"	"	Simulation	N/A	7.1
"	"	Infinite	7.1	9.0

plate. On the other hand, the moment resisting capacity of the sandwich plate element is exhausted once the cover plates reach the state of initial yield.

As the ultimate loads predicted by the sandwich model are significantly lower than those predicted by the elasto-plastic model, and the sandwich model does not adequately represent the load-deformation history of a real plate in bending, this model will not be used. Instead, the more accurate elasto-plastic element developed earlier will be utilized in all subsequent analyses.

Elastic-Plastic Analyses with Various Boundary Restraints

A series of six computer analyses were carried out with the elasto-plastic element using four and eight inch tension plates in order to evaluate the stiffening effect caused by a lengthening of the connection plate. Bounding solutions featuring no flange restraint and infinite flange restraint were obtained in addition to the more realistic solution using the flange element.

Load versus deflection at the centerline of the tension plate for various flange restraints used in the model are shown in Figure 3.5. The deflections predicted using the flange simulation model lie between those computed by no flange and infinite flange restraint models throughout the plastic load history as expected. However, it should be noted that the loads predicted with the flange simulation are much closer to those calculated without any flange restraint throughout most of the loading. As noted earlier in Figure 3.3, the flange simulation model yields quite accurate load-deflection behavior. Consequently, one could assume no flange restraint for a reasonable estimate of the load-deflection behavior. It can be seen in Figure 3.5 that the loads predicted by a no flange restraint model are always lower than those obtained with flange simulation.

The development of plastic regions in the web are shown in Figures 3.6 through 3.11. Figures 3.6 and 3.9 (no flange restraint) and Figures 3.7 and 3.10 (flange simulation) show that the plastic regions develop progressively around the tension plate only. The incremental solution can be continued without any difficulty until a wide area of plasticity has developed around the tension plate. Instability of the solution begins to occur once the plastic regions have progressed sufficiently far towards the flanges. It should be noted that no elastic regions are contained within a closed plastic zone at the apparent collapse.

Figures 3.8 and 3.11 (infinite flange restraint) show that the plastic regions develop around the tension plate and along the

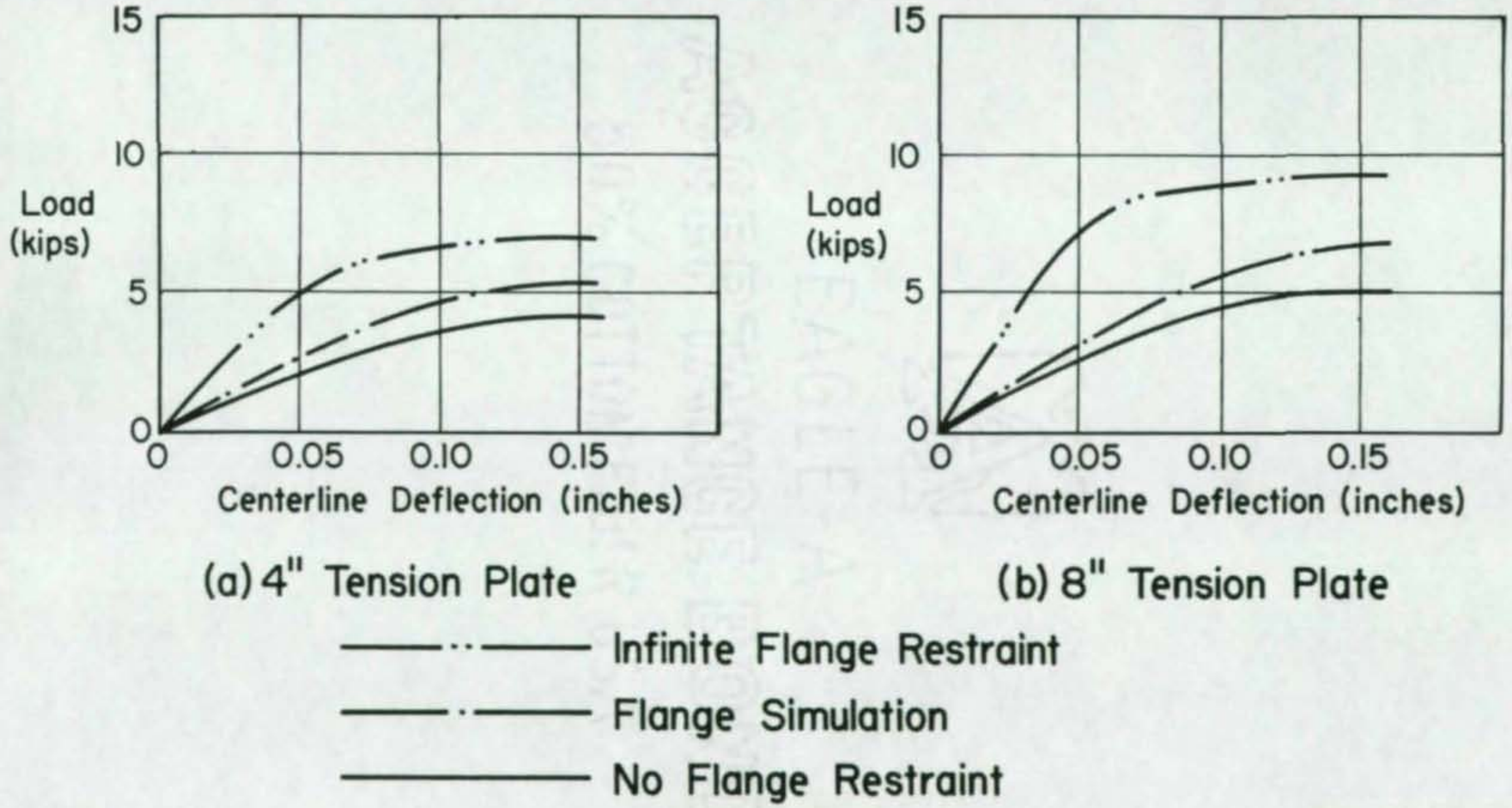

Figure 3.5. Load-Deflection Curves for Various Flange Restraints

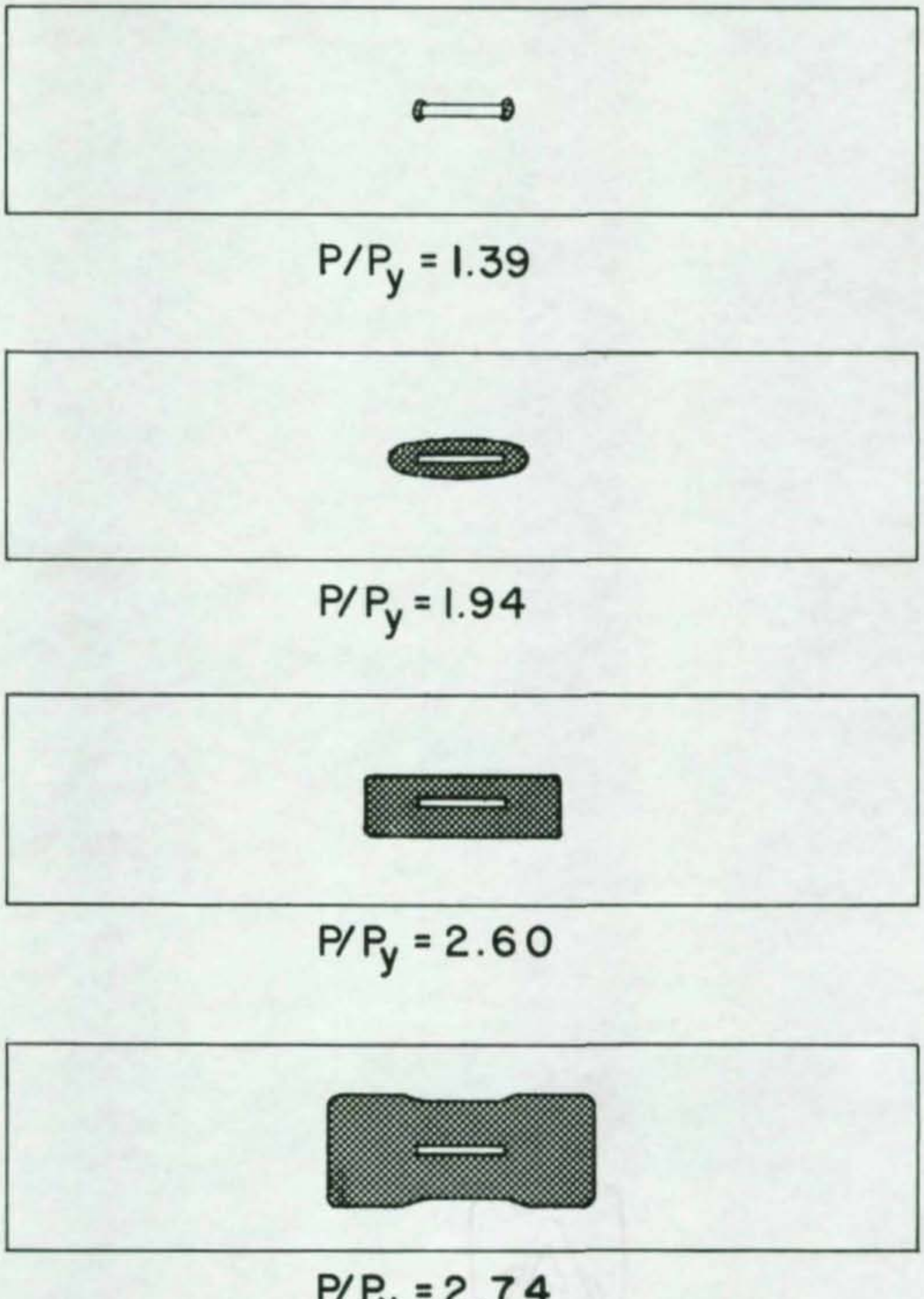

Figure 3.6. Yield Zones at Various Loads for a 4" Tension Plate and No Flange Restraint
P_y = 1.49 kips

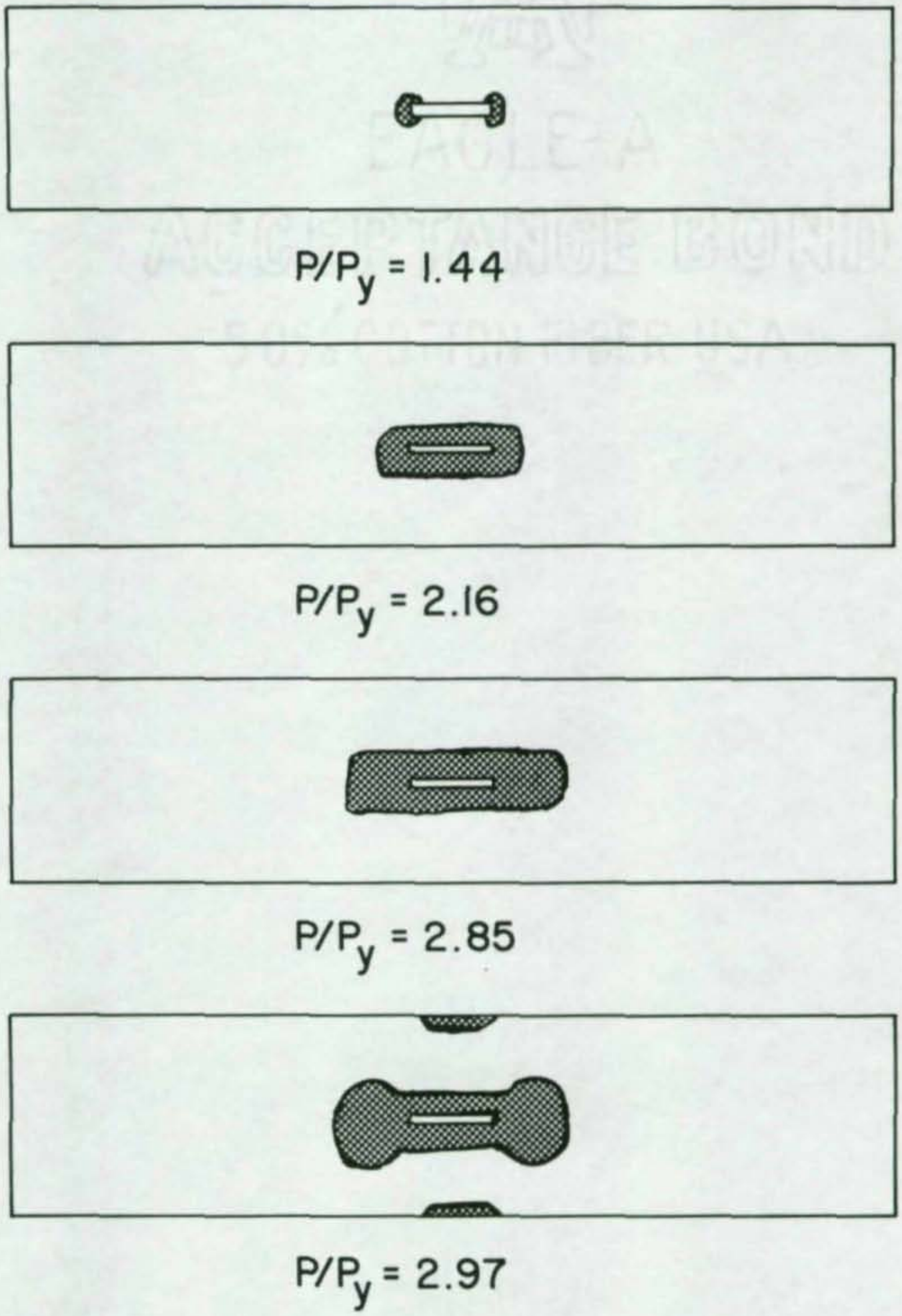

Figure 3.7. Yield Zones at Various Loads for a 4" Tension Plate with Flange Simulation
P_y = 1.82 kips

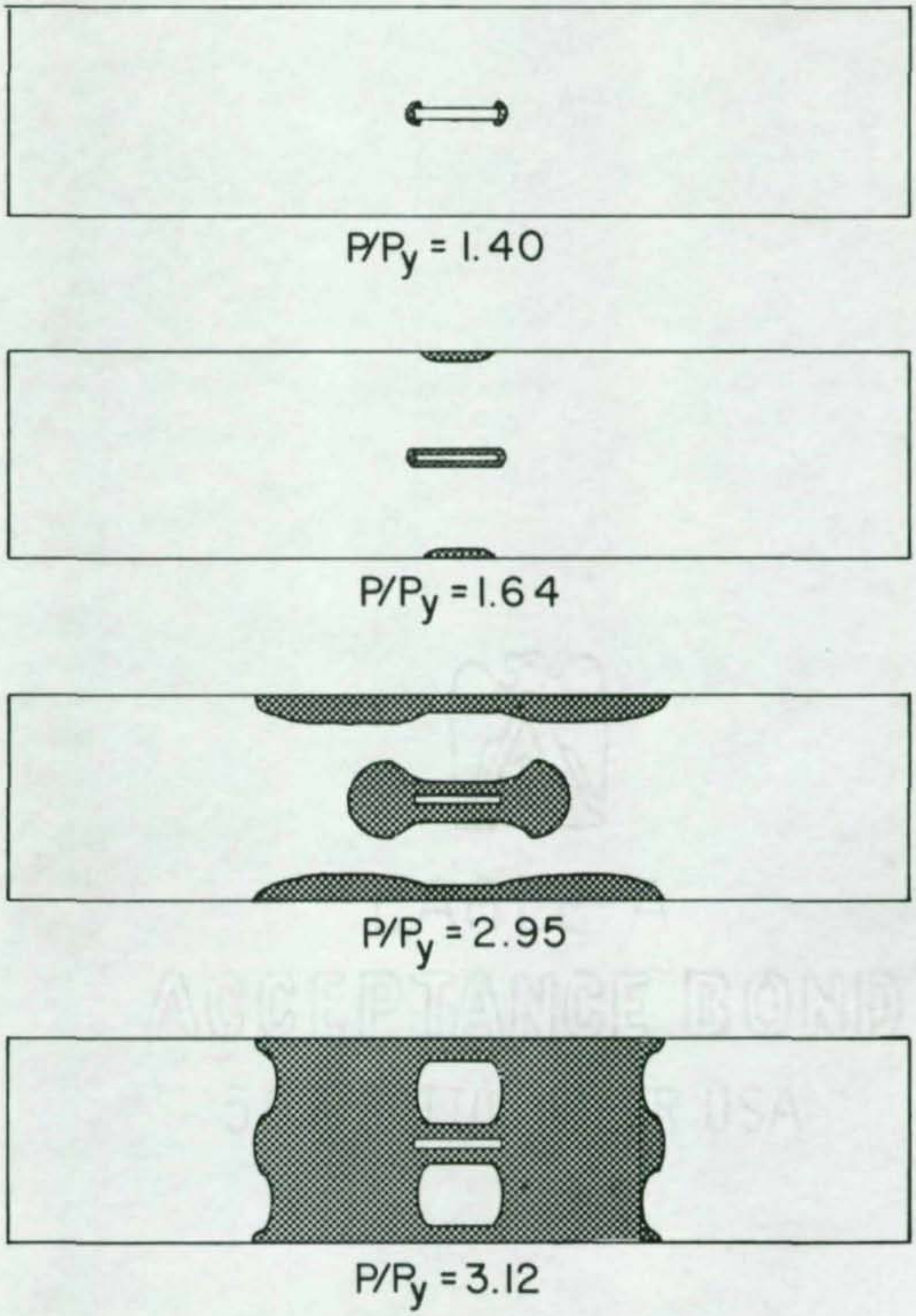

Figure 3.8. Yield Zones at Various Loads for a 4" Tension Plate and Infinite Flange Restraint
P_y = 2.26 kips

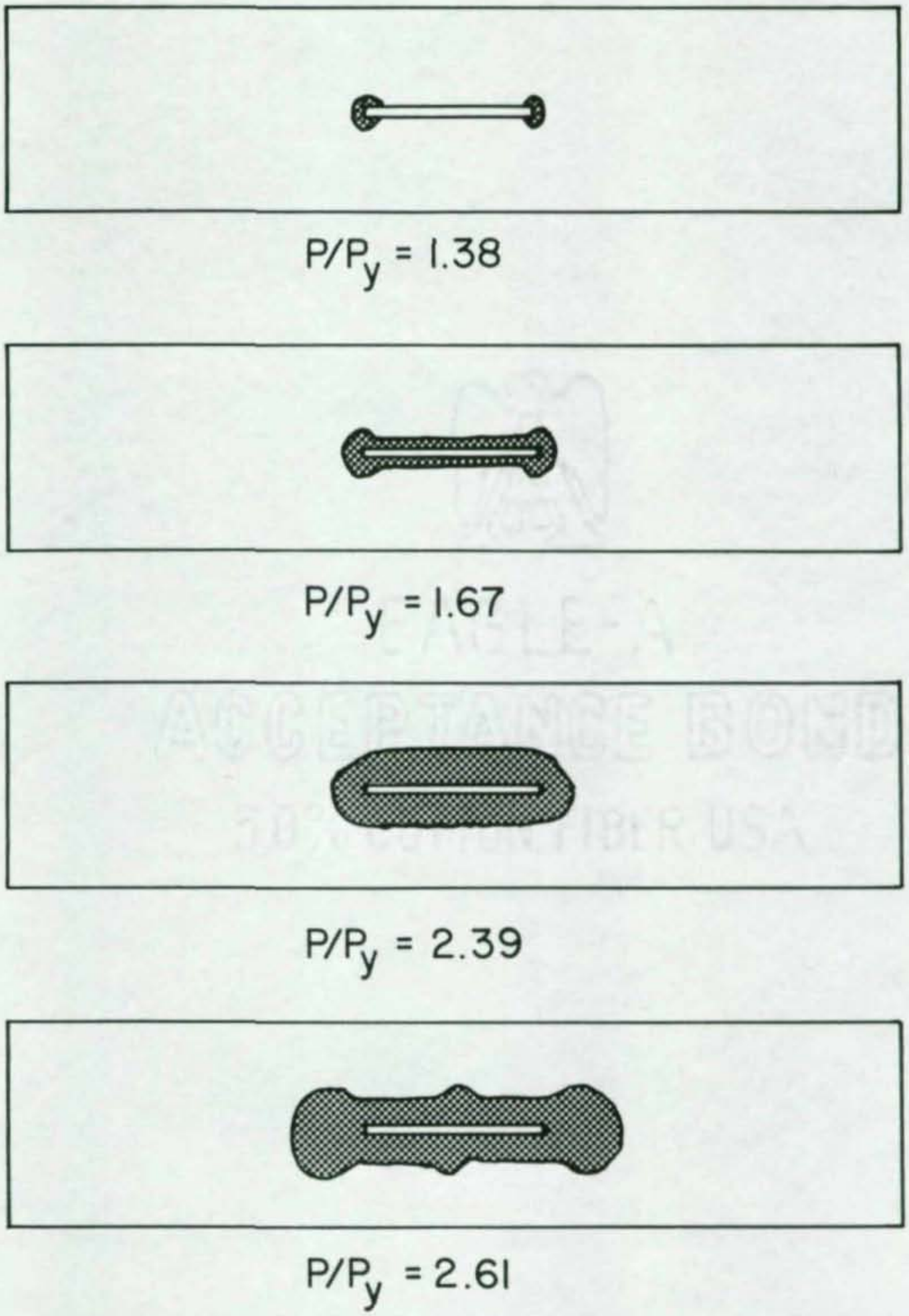

Figure 3.9. Yield Zones at Various Loads for a 8" Tension Plate and No Flange Restraint
P_y = 1.92 kips

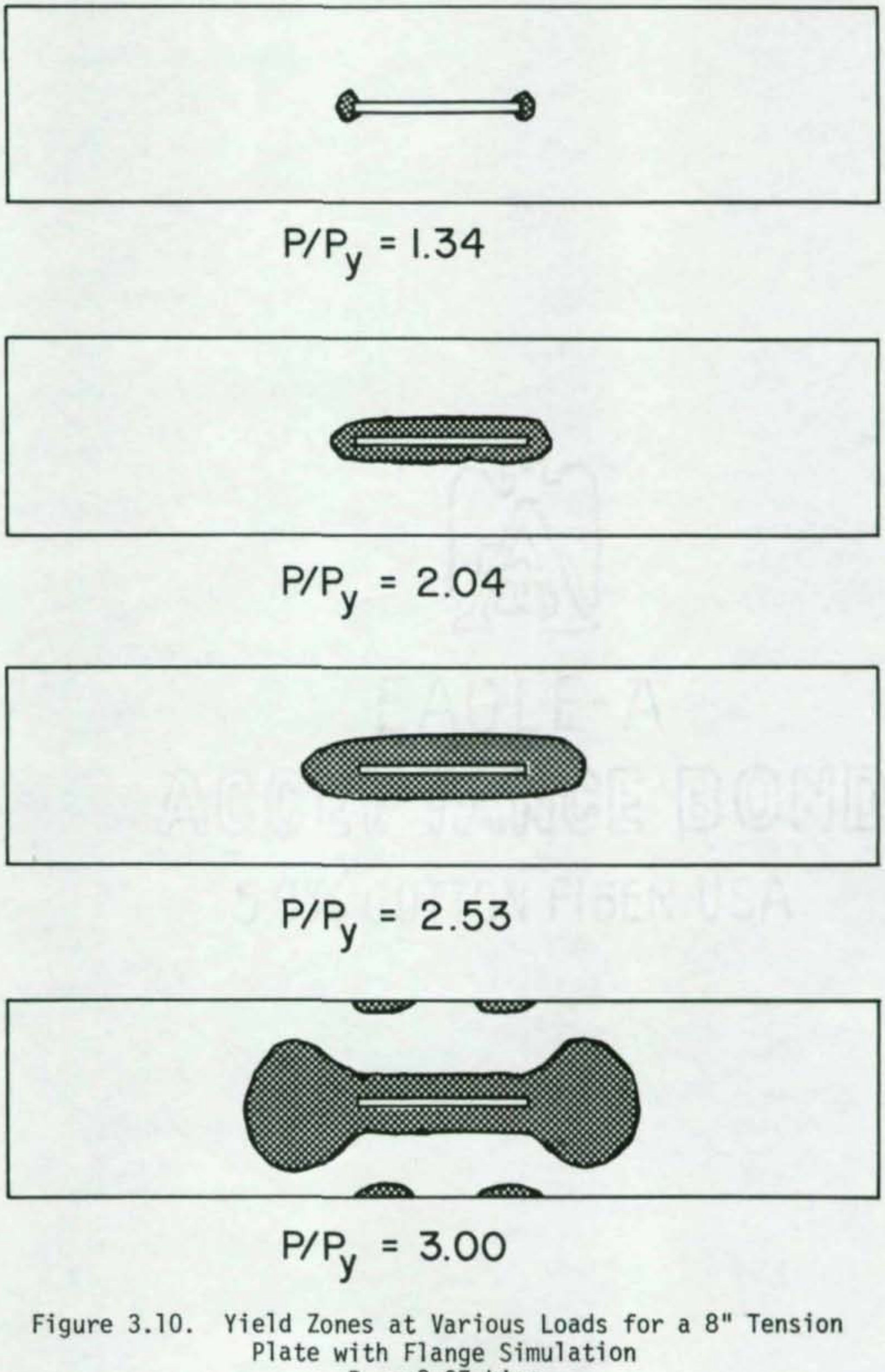

Figure 3.10. Yield Zones at Various Loads for a 8" Tension Plate with Flange Simulation
P_y = 2.37 kips

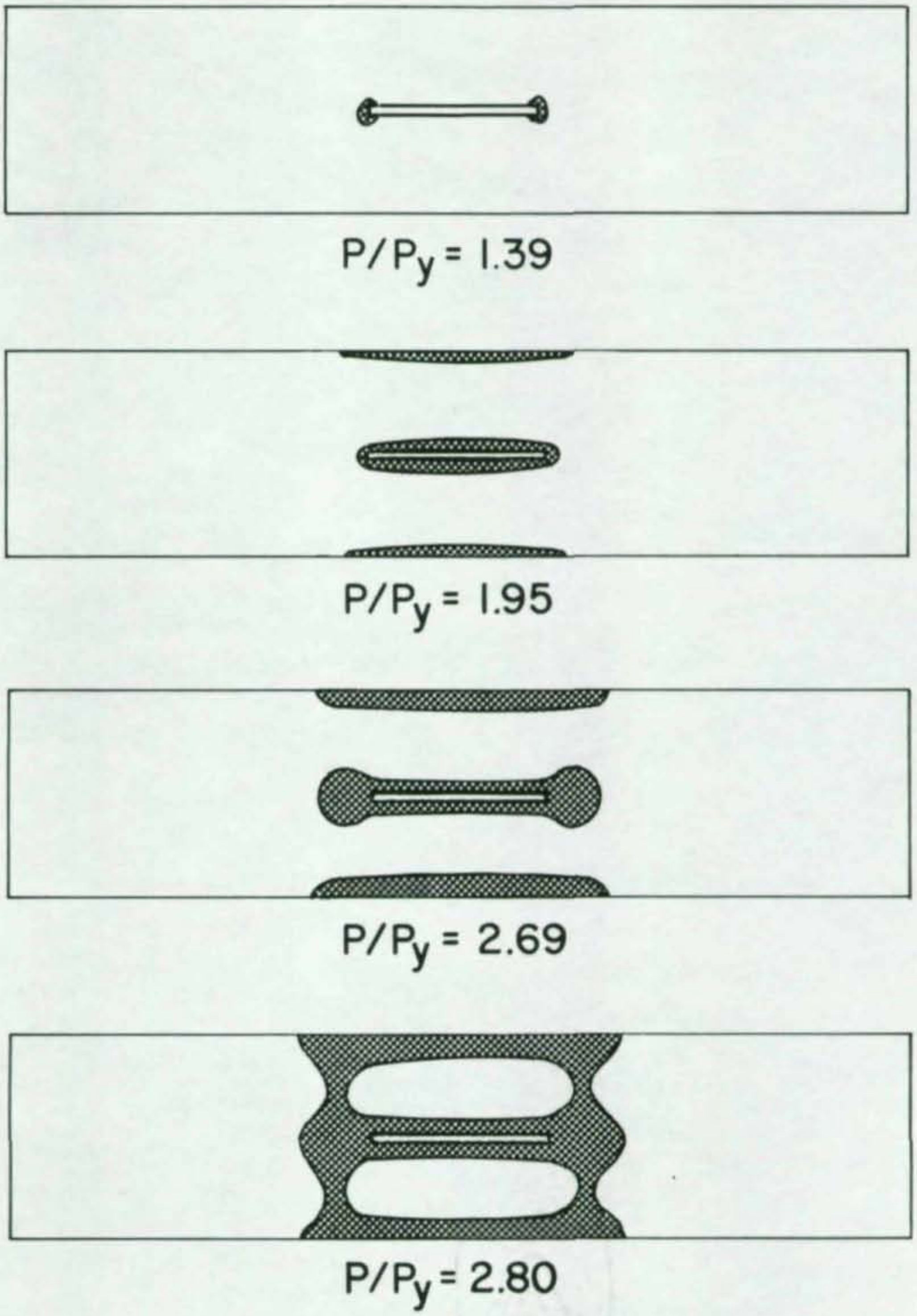

Figure 3.11. Yield Zones at Various Loads for a 8" Tension Plate and Infinite Flange Restraint
P_y = 3.20 kips

web-flange juncture simultaneously. As loading progresses, the two areas of plasticity extend towards each other, eventually joining together prior to reaching the collapse load. It should be noted that these plastic extensions enclose areas of elastic material which are located between the tension plate and the flanges.

Note that plasticity does not develop along narrow lines, as is assumed in the yield line theory, rather, the plastic regions extend in broad areas. An examination of the computer output suggests that this is due to an interaction of the shearing and large normal stresses which develop at the ends of the tension plate. On the other hand, along the sides of the tension plate and the web-flange juncture, yielding develops in thin bands as assumed in the yield line theory.

Finally, a comparison of the load-deflection curves for the flange simulation cases indicates that a doubling of the tension plate width reduces the deflection by only approximately 16%. The corresponding collapse load increases by 31%.

CHAPTER IV

COMPARISON OF ANALYTICAL AND EXPERIMENTAL RESULTS

As noted in Chapter I, past design practice has been to simply size the tension plate to support the tensile load and assume that the member web could transfer the load. However, Csernak (6) has shown that, if the web is not stiffened, excessive deformation of the web will occur and the flange would undergo large rotation at design loads. In addition, it was found that the failure will always occur in the web. An analysis technique for stress and deflection calculations in the web, thus, becomes a necessity.

There are two design techniques that are currently used in the analysis of these web connections. The first is an elastic method suggested by Blodgett (1), and the second, a plastic or ultimate strength yield line technique proposed by Kapp (5). Both of these methods are described and discussed in the following sections.

Elastic Method

As shown in Figure 4.1 (b), Blodgett assumes that the tensile load, P, produces a uniform stress under the tension plate that dies out linearly from the ends of the tension plate at a distance of twelve times the web thickness. This produces a force per unit width of the web which may be easily computed and is given by

$$f = \frac{P}{d + 12h} \quad . \tag{4.1}$$

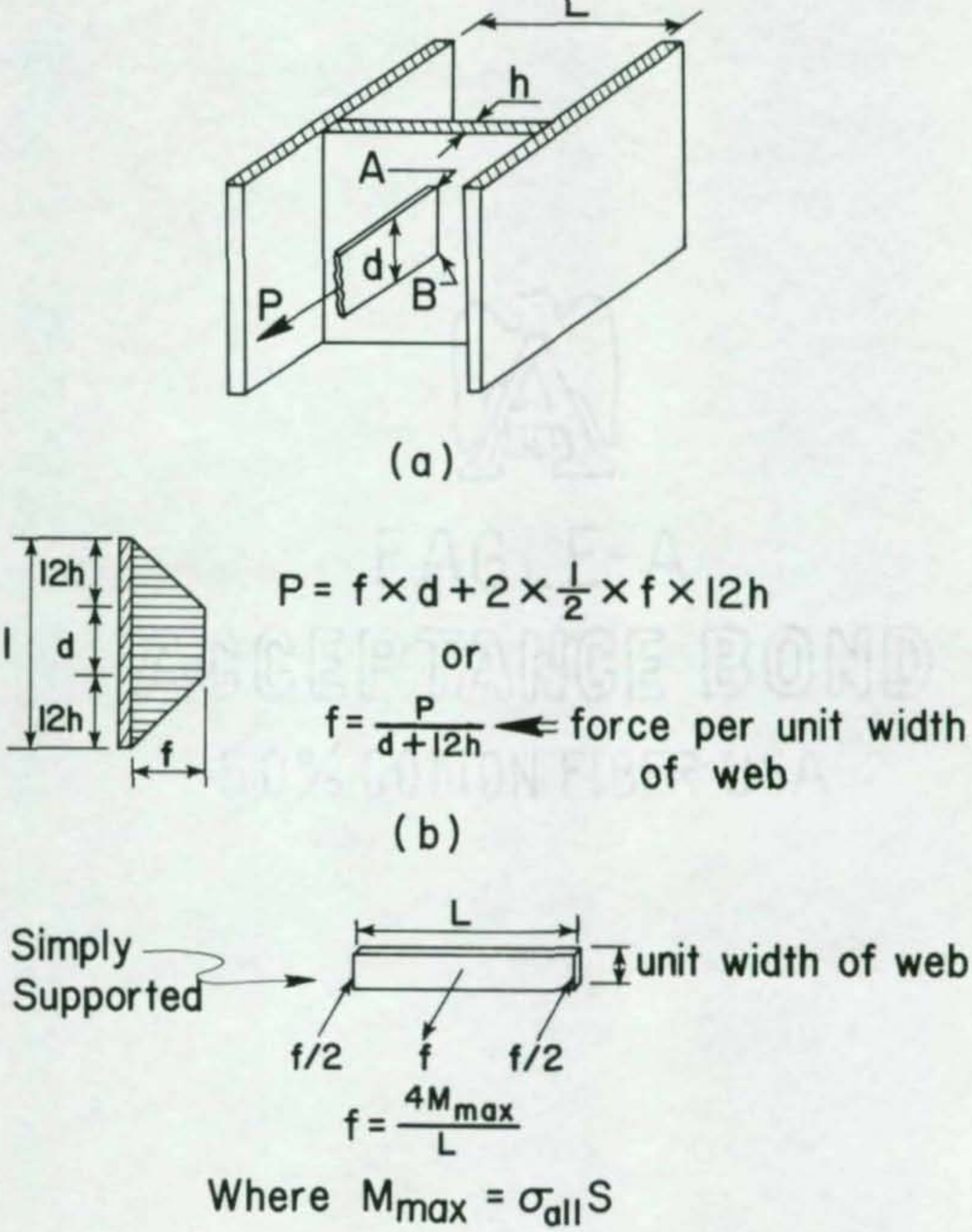

Figure 4.1. Elastic Analysis as Proposed by Blodgett

By assuming that the flanges provide no restraint, a unit width of the web can be analyzed as a simply-supported beam subjected to a concentrated load at mid-span. The maximum force, f, can be determined by calculating the value of the maximum moment that a unit width of the web cross-section can support. This is given by

$$f = \frac{4\,\sigma_{all}S}{L} \quad . \tag{4.2}$$

in which σ_{all} is the allowable stress and S is the section modulus for a unit width of the web. Equating Equations (4.1) and (4.2) leads to the value of the maximum allowable load, P, which is found to be

$$P = \frac{2}{3}\,\frac{(d + 12h)}{L}\,\sigma_{all}h^2 \quad . \tag{4.3}$$

The bounding solution for infinite flange restraint can be easily found by noting that the maximum bending moment for full-fixity is one-half that of the simply-supported case. Therefore, a simple doubling of Equation (4.3) will give the allowable load for this connection assuming infinite flange restraint.

Comparison with Computer Solution

This design procedure has two inherent shortcomings. The first concerns the assumed load distribution in the web. Previous finite element studies (6) have shown that large stress concentrations exist at points A and B in Figure 4.1 (a). This could be viewed as if concentrated loads are being applied to the web at points A and B (2) which could result in a reduction of the permissible load. However, because of the highly localized nature of the stress concentrations, rapid dissipation of the large stresses according to St. Venant's principle occurs. Therefore, this phenomena of stress concentration can be neglected especially in light of the inherent ductility of the connection materials.

The second shortcoming concerns the simplifying assumption that the web can be analyzed as a one-dimensional beam rather than as a two-dimensional plate. This is a conservative assumption. The beam solution approaches the two-dimensional plate solution as the length of the connection plate increases. An examination of the last two columns of Table 4.1 indicates that as the tension plate length increases, the initial yield load predicted by the Blodgett's elastic solution approaches the more accurate computer solution. Due to an increase in the length of the plate, the load is distributed more uniformly to the web and the effect of the stress concentrations at the ends of the plate is reduced. Additionally, an increase in the flange restraint along the edges of the web, along with an increase in the plate length, reduces the amount of web curvature in the longitudinal direction. As such, the Poisson effect is reduced and beam bending, rather than plate bending, becomes more pronounced. Overall, though, the general result of the procedure is an underestimation of the initial yield load.

Yield Line Method

The yield line method, as proposed by Kapp (5), is an upper-bound limit analysis procedure that depends on a proper yield pattern assumption for its accuracy. The yield line pattern assumed for this connection is shown in Figure 4.2. By assuming that the parts of the web contained within the yield lines rotate as rigid bodies, the internal work is exclusively done along the yield lines and is given for a unit length by the product of the uniform plastic moment ($M_p = \sigma_o h^2/4$) and the corresponding rotation (as measured normal to the

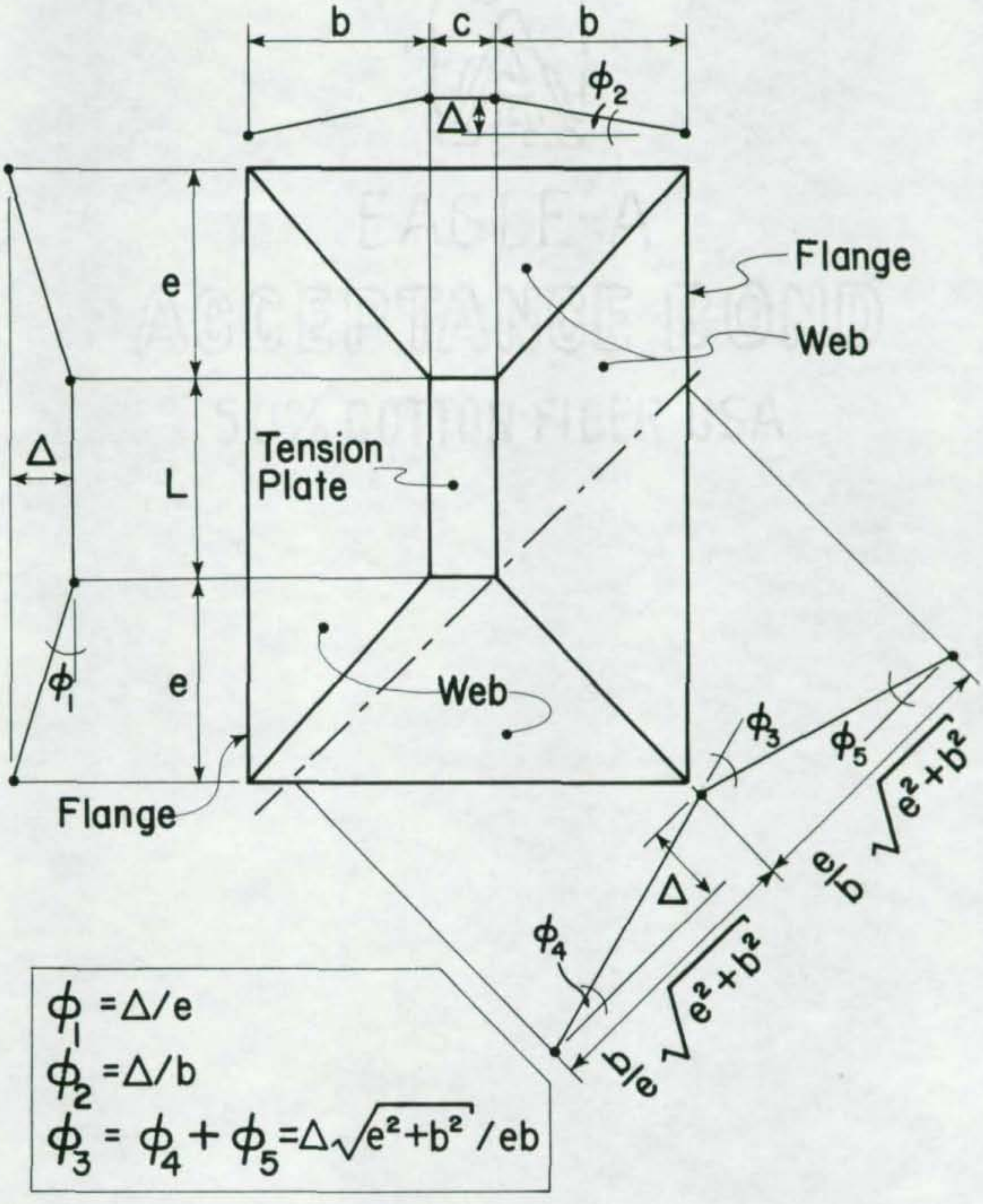

Figure 4.2. Yield Line Pattern for the Light Bracing Connection

Table 4.1. Comparison of Ultimate Loads Using Various Solution Techniques

Member	Tension Plate	Flange Restraint	Ultimate Load (kips)		Initial Yield Load (kips)	
			Computer Solution	Yield Line Solution	Computer Solution	Blodgett's Elastic Solution
W10x21	4"	None	4.1	7.0	1.5	1.0
"	"	Simulation	5.4	---	---	---
"	"	Infinite	7.0	10.5	2.3	2.0
"	8"	None	5.0	8.0	1.9	1.6
"	"	Simulation	7.1	---	---	---
"	"	Infinite	9.0	12.4	3.2	3.2

yield lines). From the virtual work principle, summing internal energy and equating to the external work done by the collapse load, P_u, results in an expression for the value of P_u in terms of the geometry of the yield pattern and the geometric and material properties of the web.

Referring to Figure 4.2, and assuming that the flanges provide no restraint to the web, summation of the internal energy along the yield lines results in

$$W_i = \frac{\psi}{4} [2 (2b + 2c) \phi_1 + 2L\phi_2 + 4 \sqrt{e^2 + b^2} \phi_3] \quad , \tag{4.4}$$

in which $\psi = \sigma_o h^2$. The corresponding external work performed by the ultimate load, P_u, is given by

$$W_e = P_u \Delta \quad . \tag{4.5}$$

In Equation (4.4), the internal energy is seen to be a function of a variable length, e, along the flanges, as shown in Figure 4.2. By minimizing the work done by the plastic moment along the yield lines, a relationship can be determined for the smallest load that will result in a failure mechanism of the web. Thus, differentiating Equation (4.4) with respect to e and equating to zero leads to

$$e = b\sqrt{2 + c/b} \quad . \tag{4.6}$$

Equating internal and external energies [Equations (4.4) and (4.5)] and utilizing Equation (4.6) results in

$$P_u = \psi\, L/2b + 2\psi\sqrt{2 + c/b} \quad . \tag{4.7}$$

By a similar procedure, the ultimate load corresponding to the bounding solution for infinite flange restraint can be shown to be given by

$$P_u = \psi L/b + 4\psi\sqrt{1 + c/2b} \quad . \tag{4.8}$$

Because this is an ultimate strength criteria, a reduction in the computed load is necessary to obtain the working load. Load reduction factors of 1.7 for live and dead loads or 1.3 for these loads acting in conjunction with wind loads are the recommended practice (17).

Comparison with Computer Solution

The results obtained from the elasto-plastic computer solution for various tension plate lengths and boundary restraints are shown in Table 4.1 along with the corresponding yield line solutions. It can be seen that the yield line theory predicts ultimate loads that are much greater than those given by the computer solution.

The energy approach used in the yield line theory gives an upper-bound solution whereas the computer solution, which is an equilibrium solution, renders a lower-bound solution (9). Therefore, a difference between the results obtained by the two solution schemes is to be expected. It may be emphasized that the incremental elastic-plastic computer solution using the tangent modulus approach, as presented in this study, always satisfies the yield condition due to the utilization of the Newton-Raphson iteration technique. In addition, the choice of the displacement field in finite elements used in this development is such that convergence to a correct solution is guaranteed with decreasing mesh size. Therefore, the computer solution, as presented, closely approximates the correct behavior within the small deflection range. Thus, the discrepancy between the yield line solution and the corresponding computer solution is attributable to the errant assumption of the formation of narrow plastic zones along the yield lines. In fact, the plasticity in the web develops in broad areas, as can be seen in Figures 3.6 through 3.11.

Experimental Results

The discussion above indicates reasons for the discrepancy between the yield line theory and the computer results. However, the question of why the experimentally obtained values of the collapse loads for these connections are much greater than even the upper-bound ultimate loads predicted by the yield line theory remains unanswered (6).

Although the yield line theory assumes that deflections are small, application of design loads based upon a yield line analysis can lead to relatively large deflection. Large deflections (i.e., displacements greater than one-third to one-half the plate thickness) are known to induce tensile membrane stresses which significantly increase the strength of a plate made of a ductile material. As an example, the yield line load of 7.0 kips for a 4" tension plate from Table 4.1 results in a factored load of 7.0/1.7 = 4.1 kips. For this design load, the resulting deflection from Figure 3.5 (a) is found to be approximately equal to 0.16", which is 2/3 the thickness of the web plate (0.24"). A consequence of this large deflection is that the web experiences an increase in load-carrying capability as a result of the induced membrane action, which is much more efficient in supporting loads than the bending action.

Csernak (6) has developed an empirical relationship which predicts the ultimate strength of the light bracing connection shown in Figure 3.1. This relationship is given by

$$P_u = \sigma_o h \ (0.33L + 0.30d) \quad , \tag{4.9}$$

where L is the depth of the wide-flange section and d is the length of the tension plate. This equation is based on 20 tests of various wide-flange sections having 4", 6" and 8" tension plates. The interesting aspect of Equation (4.9) concerns the linearity of the ultimate load with respect to the web thickness. This indicates that membrane action is the principle load transfer mechanism at load levels corresponding to collapse loads. Csernak also observed large deflections at collapse loads in his experiments, which justifies the linearity of Equation (4.9) with respect to web thickness, h.

For W10x21 with 4" and 8" tension plate connections, for which elastic and yield line solutions have been shown in Table 4.1, ultimate loads computed by the empirical Equation (4.9) are equal to 38.9 and 49.2 kips, respectively. These ultimate loads are approximately four times larger than those given by the yeild line method, thereby, indicating the additional load-carrying capacity at collapse due to membrane action.

Evaluation and Recommendations

Based upon the experimental and analytical evidence presented in this study, the yield line theory has been shown not to be applicable to the connection group studied in this report. Computer results have shown that the assumption of narrow yield lines is incorrect. In addition, experimental data indicates that membrane rather than bending action prevails as the principle means of load transfer, which results in limit loads that are significantly higher than those predicted by the yield line theory.

Although the application of the yield line method is seen to lead to conservative estimates of the ultimate strength of these connections, use of the design loads determined by the yield line theory leads to excessively large deflections in the web as shown in the previous section. This behavior, in conjunction with the resulting large flange rotations, could cause local buckling failure of the web.

Web deflections can be reduced by lengthening the tension plate, but this is of dubious value. It has been seen that even a doubling of the plate length reduces the deflections by only 16% for the W10x21 section. As such, the use of web doubler plates, Tee sections or stiffners is highly recommended.

For connections with unstiffened webs, the design loads must be kept at a fairly low level in order to avoid excessive deflections in the web. Initial yield loads predicted by the Blodgett's elastic method provide reasonably accurate estimates when compared with the computer solution and are relatively low in magnitude. Web deflections due to these loads remain within the small deflection range. Consequently, loads obtained by the Blodgett's method provide safe and conservative values for the design loads in light bracing connections of the type discussed in this study.

It should be emphasized, however, that for those connections where excessive deflections are of minor concern, design loads can be estimated based on yield line theory. Although relatively large in magnitude compared to those calculated by the Blodgett's elastic method, these design loads still provide a large margin of safety to ultimate loads determined experimentally. An estimate of the ultimate loads can be made by using the experimentally obtained empirical Equation (4.9). These loads are approximately two to four times larger than the corresponding loads determined by the yield line method. It should be noted that web deflections at these loads are extremely large due to the ductility of the connection materials.

CHAPTER V

CONCLUSIONS AND SUGGESTIONS FOR FURTHER RESEARCH

Conclusions

An elastic-plastic finite element analysis of the simple tensile connection shown in Figure 3.1 has been performed using a specially formulated elasto-plastic plate bending element. Comparisons of the results using sandwich plate elements proposed earlier by other researchers (14, 15) indicates that the sandwich element traces the development of the plastic regions quite well but significantly underestimates the collapse load. Therefore, the element developed in this study is recommended for correct estimates of the elastic-plastic load history in plate bending problems.

Various tensile connections with different tension plate widths were analyzed using the elasto-plastic element developed in this study. It is found that yielding develops in broad regions, and not along narrow yield lines as assumed in the yield line theory. Consequently, the yield line theory is not strictly applicable to this connection type.

The computer results of the various finite element analyses within the elastic range were compared against the corresponding results of the approximate elastic method proposed by Blodgett (2). In each case, it was found that the initial yield loads determined by the two methods were reasonably close to each other. Blodgett's method can, therefore, be used to obtain reliable estimates of the initial yield load within the small deflection range.

Experimental data given by Csernak (6) indicates that the deflections for such connections at collapse loads are excessively large and are well beyond the range of the small deflection theory. Consequently, membrane rather than bending action predominates in the web resulting in much higher collapse loads compared to those predicted by the yield line method, which is based on the small deflection theory.

Although the yield line method assumes small deformations, collapse loads computed with this theory, when applied to the elasto-plastic finite element model, yield deflections that are outside the small deformation range. In fact, deflections at even design loads (i.e., yield line collapse loads/1.7) are large enough to be outside the small deflection range. Hence, it can be reiterated that the yield line theory is not applicable for the connections considered in this study.

Based upon the aforementioned findings, the following recommendations can be made for the design of these tensile web connections:

1. Where the deflections must remain within the small deformation range, Blodgett's elastic method can be used to obtain safe and reliable design loads.

2. Where the deflections are of minor concern, Kapp's yield line method can be utilized to obtain design loads.

3. Large deflections at design loads computed by the yield line theory can be avoided by using stiffeners, doubler plates or Tee sections.

4. The actual ultimate loads determined experimentally can be predicted by using the empirical Equation (4.9), which gives values that are two to four times larger than those obtained by the yield line theory. Therefore, a quick and conservative

estimate of the yield line collapse load can be achieved by dividing the values obtained from Equation (4.9) by a factor of 4.

Suggestions for Further Research

The analytical research reported herein represents only an initial investigation. Further research should include:

1. Extension of the work to the large deformation range.
2. Expansion of the capacity of the existing program to include three-dimensional capabilities in order that the effect of doubler plates and stiffeners can be evaluated.
3. Determination of a more realistic and rational basis for the analysis of these types of connections.

APPENDICES

Appendix A

Rectangular Element Stiffness Matrix

The rectangular element stiffness matrix can be expressed in general form by use of Equation (2.17). This can be written as

$$[k] = \Omega\,[C]^{-T} \int_{\text{area}} [Q]^T\,[D]\,[Q]\,dA\,[C]^{-1} \quad , \tag{A.1}$$

in which Ω is the rigidity term that is equal to $h^3/12$ for the elastic element, and is given by Equations (2.38) and (2.39) for the plastic element. Matrix [C] is given by Equation (2.4), so it only remains to evaluate the integral in Equation (A.1). By making use of the partitioned matrix representation for [Q], as given by Equation (2.10), and performing the indicated triple matrix multiplication, the integrand is expressed as

$$[Q]^T\,[D]\,[Q] = \begin{bmatrix} [Q_0]^T\,[D]\,[Q_0] & [Q_0]^T\,[D]\,[Q_1] & [Q_0]^T\,[D]\,[D_2] \\ [Q_1]^T\,[D]\,[Q_0] & [Q_1]^T\,[D]\,[Q_1] & [Q_1]^T\,[D]\,[Q_2] \\ [Q_2]^T\,[D]\,[Q_0] & [Q_2]^T\,[D]\,[Q_1] & [Q_2]^T\,[D]\,[Q_2] \end{bmatrix} . \tag{A.2}$$

All triple matrix products containing $[Q_0]$ and $[Q_0]^T$ terms are null matrices. Also, because $[Q_2]^T\,[D]\,[Q_1]$ is the transpose of $[Q_1]^T\,[D]\,[Q_2]$, only three of the submatrices need to be evaluated.

The matrix represented by $[Q_1]^T\,[D]\,[Q_1]$ is a constant matrix and, as such, its integration involves only multiplication by the area of the element, i.e.,

$$\int_{\text{Area}} [Q_1]^T\,[D]\,[Q_1]\,dA = 4 \times \text{Area} \begin{bmatrix} D_{11} & -D_{13} & D_{12} \\ & D_{33} & -D_{23} \\ \text{SYM.} & & D_{22} \end{bmatrix} . \tag{A.3}$$

For the remaining integrations, the following formulas are required. Referring to Figure 2.1,

$$\iint dxdy = \text{Area} = ab \quad , \qquad \iint x^2 y\,dxdy = 0,$$
$$\iint x\,dxdy = 0 \quad , \qquad \iint xy^2 dxdy = 0,$$
$$\iint y\,dxdy = 0 \quad , \qquad \iint x^3 dxdy = 0,$$
$$\iint x^2 dxdy = \frac{a^3 b}{12} \quad , \qquad \iint y^3 dxdy = 0,$$
$$\iint xy\,dxdy = 0 \quad , \qquad \iint x^4 dxdy = \frac{a^5 b}{80} ,$$
$$\iint y^2 dxdy = \frac{ab^3}{12} \quad , \qquad \iint y^4 dxdy = \frac{ab^5}{80} ,$$
$$\iint x^2 y^2 dxdy = \frac{a^3 b^3}{144} \quad , \qquad \iint x^3 y\,dxdy = 0 ,$$
$$\iint xy^3 dxdy = 0 \quad . \tag{A.4}$$

The integration of $[Q_1]^T\ [D]\ [Q_2]$, then, results in

$$\int [Q_1]^T\ [D]\ [Q_2]\ dA = \begin{bmatrix} 0 & 0 & 0 & 0 & -D_{13}a^3 b & -D_{13}ab^3 \\ 0 & 0 & 0 & 0 & D_{33}a^3 b & D_{33}ab^3 \\ 0 & 0 & 0 & 0 & -D_{23}a^3 b & -D_{23}ab^3 \end{bmatrix} . \tag{A.5}$$

Similarly, performing the indicated triple product $[Q_2]^T\ [D]\ [Q_2]$ and integrating yields the following

$$\begin{bmatrix} 3D_{11}a^3 b & 0 & 0 & 0 & 0 & 0 \\ & \frac{1}{3} D_{11}ab^3 + \frac{4}{3} D_{33}a^3 b & -\frac{2}{3} D_{23}a^3 b - \frac{2}{3} D_{13}ab^3 & D_{12}ab^3 & 0 & 0 \\ & & \frac{1}{3} D_{22}a_3 b + \frac{4}{3} D_{33}ab^3 & -2\ D_{23}ab^3 & 0 & 0 \\ & & & 3D_{22}ab^3 & 0 & 0 \\ & \text{SYMMETRIC} & & & \frac{1}{4} D_{11}a^3 b^3 + \frac{9}{20} D_{33}a^5 b & \frac{1}{4} D_{12}a^3 b^3 + \frac{1}{4} D_{33}a^3 b^3 \\ & & & & & \frac{1}{4} D_{22}a^3 b^3 + \frac{9}{20} D_{33}ab^5 \end{bmatrix} . \tag{A.6}$$

With these explicit expressions for the integration of the triple matrix products of Equation (A.2), the stiffness matrix for the rectangular element can be easily calculated. By leaving the constitutive matrix in general form, the elastic or incremental elasto-plastic stiffness matrices can be determined by simple substitution of the appropriate constitutive relationships.

Appendix B

Newton-Raphson Iteration Technique for Stress Correction

The general technique has been well described by Weisgerber (18) for the elastic-plastic finite element problem so only a short summary of the procedure is presented herein.

The technique is utilized during each load increment as outlined in the following steps.

1. Calculate incremental element stiffness matrices. For plastic elements, determine the element stiffness by using total stresses and strains of the previous load increment for calculation of the incremental plastic stress-strain relations given in Equation (2.24) and the plastic zone extent factor ϕ given by Equation (2.33).

2. Determine the smallest factored load which initiates yielding in a previously elastic element(s). Calculate incremental displacements, stresses and moments for each element. For plastic elements, determine the incremental moments by using Equations (2.36) and (2.37). The incremental stresses in the plastic part are found from the incremental curvatures at the centroid of the plastic region of the cross-section and are given by

$$\{\Delta\sigma\} = (\frac{1}{4} + \frac{\phi}{2})h[D]^p\ \{\Delta\kappa\} \quad . \tag{B.1}$$

3. Add the incremental moments, stresses and displacements to the previous total values. For each plastic element, check if the stresses exceed the yield criterion. If the equivalent stress surpasses the limiting value by more than a prescribed tolerance, corrective moments and stresses need to be determined and applied (see Appendix C for further details on this procedure).

4. Calculate the moment correction for each plastic element, as required, by the following matrix relationship

$$\{M\}^c = (1-F)\ h^2\ (\frac{1}{4} - \phi^2)\ \{\sigma\} \quad , \tag{B.2}$$

as given by Equation (C.6) in Appendix C.

5. Modify the total moments by subtracting the corresponding correction moments, given in Equation (B.2). This results in a violation of the equilibrium for each corrected element.

6. To restore equilibrium, compute balancing nodal forces for each corrected element as outlined in Appendix D. The correction loads for each element are summed together to yield a total correction force vector.

   Note that this force vector represents an equilibrating body force and in no way alters the load which has been applied to the system.

7. Apply the corrective nodal forces and determine the resulting displacements, moments and stresses. Add these to the previous values. Return to step 4 and continue the iteration until no further stress corrections are required for the plastic elements. This completes the iteration sequence.

Appendix C

Determination of Moment Corrections for Plastic Elements

Once the load increment has been determined and applied in order to initiate yielding in a previously elastic element, it might be found that the elements that are already plastic may violate the yield criterion. This exceedance needs to be corrected as described below. The von Mises yield condition is reproduced here as

$$\sigma_x^2 - \sigma_x \sigma_y + \sigma_y^2 + 3 \sigma_{xy}^2 = \sigma_o^2 \quad , \tag{C.1}$$

where σ_o = the yield stress in simple tension. If one defines

$$\begin{aligned} \alpha &= 3(\sigma_x - \sigma_y)/2\sigma_o \quad , \\ \beta &= 3 \sigma_{xy}/\sigma_o \quad , \\ \gamma &= (\sigma_x + \sigma_y)/2\sigma_o \quad , \end{aligned} \tag{C.2}$$

then, upon squaring and summing, the von Mises yield criterion can be expressed as

$$\alpha^2 + \beta^2 + \gamma^2 = 1 \quad , \tag{C.3}$$

which is the equation of a sphere (Figure C-1). If α', β' and γ' are stresses which represent a stress point outside the 'yield sphere', multiplication of α', β' and γ' by a correction factor, F, can bring the stress point onto the yield surface. This can be expressed mathematically as

$$(F\alpha')^2 + (F\beta')^2 + (F\gamma')^2 = 1 \quad , \tag{C.4}$$

from which the stress correction factor is calculated as

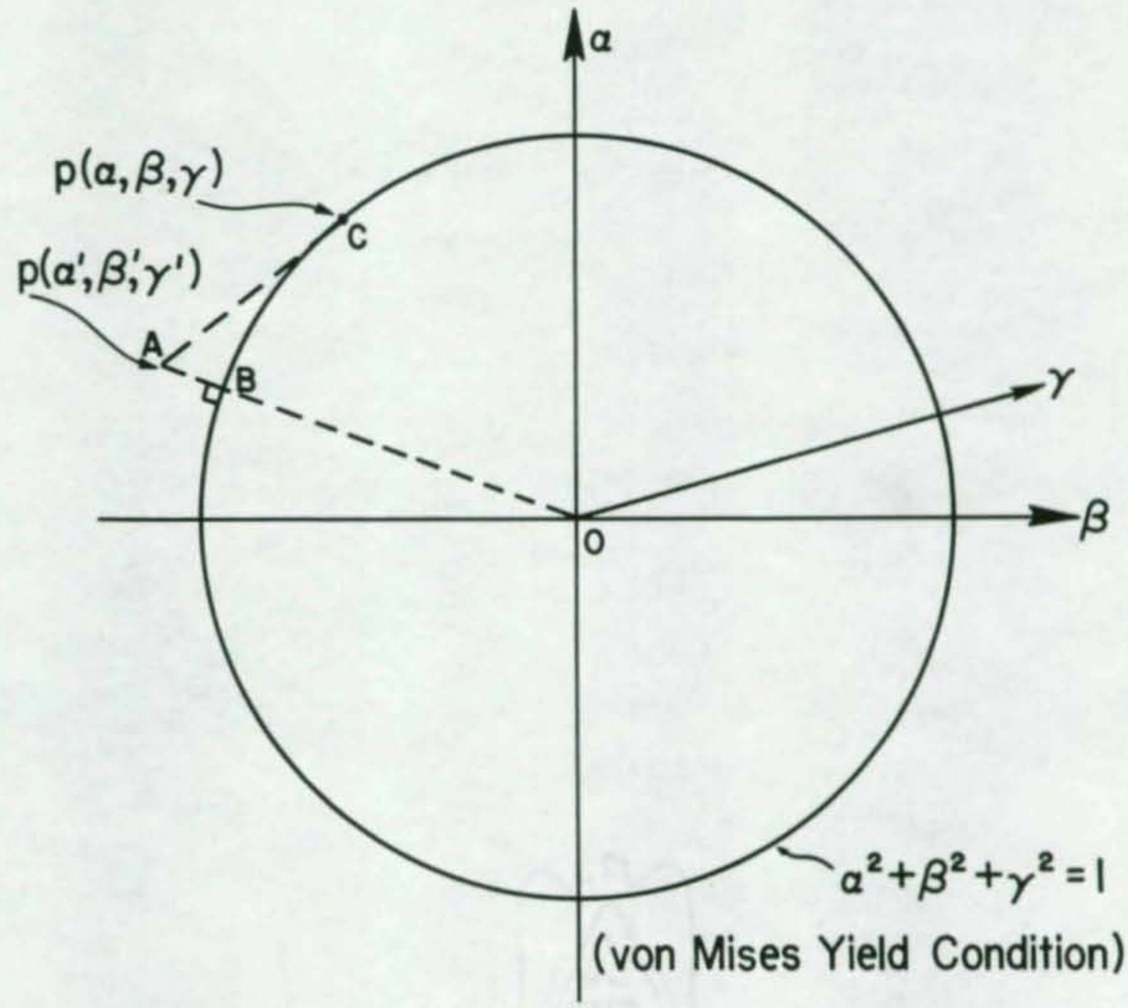

Figure C-1. Correction of Stress Point Lying Outside of Yield Sphere

$$F = (\alpha'^2 + \beta'^2 \; \gamma'^2)^{-1/2} \quad . \tag{C.5}$$

The total stresses in the plastic region of the plate cross-section, when multiplied by the stress correction factor, F, will lead to final stresses which exactly satisfy the yield condition.

To obtain the correction moments which correspond to stress corrections, the following matrix expression can be easily obtained from the stress block shown in Figure 2.4

$$\{M\}^c = h^2 \left(\frac{1}{4} - \phi^2\right) \{\sigma\}^c \quad , \tag{C.6}$$

where

$$\{\sigma\}^c = (1-F) \; \{\sigma\} \quad . \tag{C.7}$$

Appendix D

Correction Loads for Plastic Elements

As mentioned in step 6 of Appendix B, the correction loads for each plastic element may be calculated as follows.

Using Equations (2.13) and (2.15), the correction load vector can be given by

$$\{F\}^c = [C]^{-T} \int_{\text{area}} [Q]^T \{M\}^c \, dA \quad , \qquad \text{(D.1)}$$

in which the moment correction vector $\{M\}^c$, given in Equation (C.6), is taken as constant and is evaluated at the centroid of an element. Therefore, Equation (D.1) may be written as

$$\{F\}^c = [C]^{-1T} \int_{\text{area}} [Q]^T \, dA \, \{M\}^c \quad . \qquad \text{(D.2)}$$

Performing the integration on $[Q]^T$ results in

$$\int_{\text{area}} [Q]^T \, dA = \begin{bmatrix} 0 & 0 & 0 & -2A & 0 & 0 & 0 & 0 & 0 & 0 & 0 & 0 \\ 0 & 0 & 0 & 0 & 0 & -2A & 0 & 0 & 0 & 0 & 0 & 0 \\ 0 & 0 & 0 & 0 & 2A & 0 & 0 & 0 & 0 & 0 & \frac{1}{2}a^3b & \frac{1}{2}ab^3 \end{bmatrix} \quad , \qquad \text{(D.3)}$$

where A = the area of the element.

It should be noted that the application of this correction load does not constitute an additional load that is applied to the total load vector of the system. Rather, equilibrium is simply being maintained so that the true load-deflection path may be obtained by this iteration technique.

Appendix E

Elastic Stiffness for the Flange Simulation Element

This flange simulation element, as shown in Figure E-1, is a two-node beam element with torsional capability having one displacement and two rotational degrees of freedom per node. The stiffness matrix relating nodal forces to nodal displacements can be easily derived (19) and is given by

$$[K]^{local} = \begin{bmatrix} \frac{12EI}{L^3} & 0 & \frac{-6EI}{L^2} & \frac{-12EI}{L^3} & 0 & \frac{-6EI}{L^2} \\ & \frac{GJ}{L} & 0 & 0 & \frac{-GJ}{L} & 0 \\ & & \frac{4EI}{L} & \frac{6EI}{L^2} & 0 & \frac{2EI}{L} \\ & & & \frac{12EI}{L^3} & 0 & \frac{6EI}{L^2} \\ & \text{Symmetric} & & & \frac{GJ}{L} & 0 \\ & & & & & \frac{4EI}{L} \end{bmatrix} , \qquad (E.1)$$

in which I is the moment of inertia measured about the local y-y axis of the element, G is the shear modulus and J is the torsional rigidity of the element.

It should be noticed in Figure E-1 that the axes are designated as local axes for the member. The transformation of the local stiffness matrix given in Equation (E.1) to a global system can be easily performed by using the coordinate transformation expression.

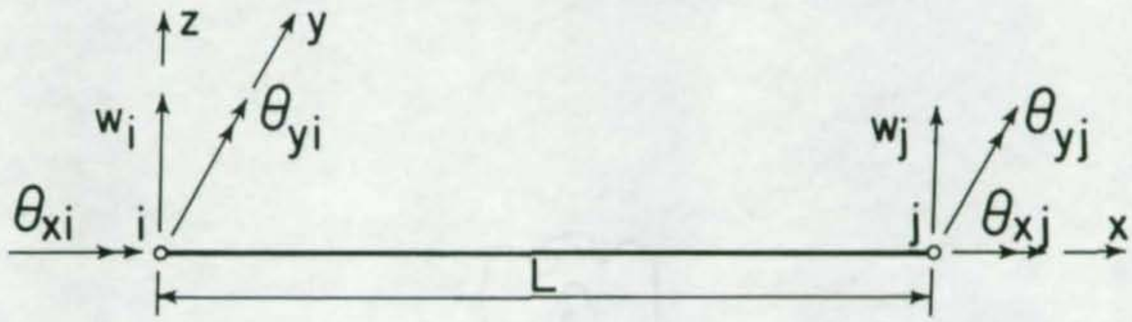

Figure E-1. Beam Element Under Combined Bending and Torsion

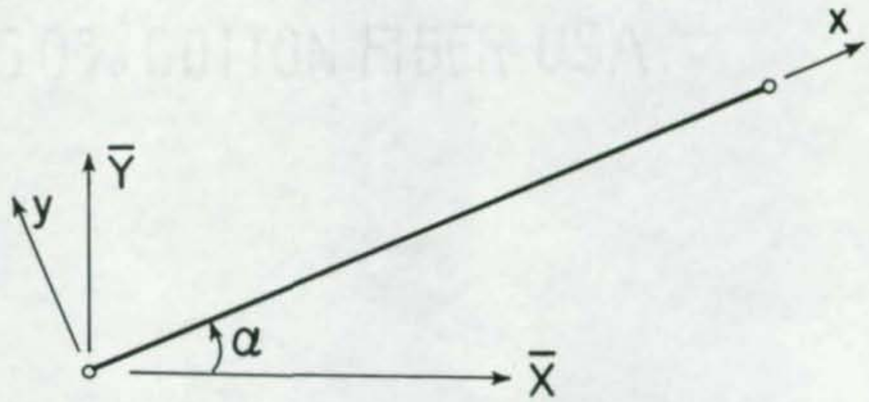

$$\theta_x = \theta_{\bar{X}} \cos\alpha + \theta_{\bar{Y}} \sin\alpha$$

$$\theta_y = -\theta_{\bar{X}} \sin\alpha + \theta_{\bar{Y}} \cos\alpha$$

Figure E-2. Transformation from Local to Global Coordinates

$$[K]^{global} = [T]^T [K]^{local} [T] \quad , \tag{E.2}$$

where

$$[T] = \begin{bmatrix} [\Lambda] & 0 \\ 0 & [\Lambda] \end{bmatrix} \quad ,$$

$$[\Lambda] = \begin{bmatrix} 1 & 0 & 0 \\ 0 & \cos\alpha & \sin\alpha \\ 0 & -\sin\alpha & \cos\alpha \end{bmatrix} \quad ,$$

and α is seen in Figure E-2 to be the angle between the global $\overline{X}$-direction to the local x-direction measured counterclockwise.

LITERATURE CITED

1. Blodgett, O. W., Design of Welded Structures, The James F. Lincoln Arc Welding Foundation, Cleveland, 1966.

2. Abolitz, A. L. and Warner, M. E., "Bending Under Seated Connections," Engineering Journal, AISC, Vol. 1, No. 1, 1965, pp. 1-5.

3. Stockwell, F. W., "Yield Line Analysis of Column Webs With Welded Beam Connections," Engineering Journal, AISC, Vol. 11, No. 1, 1974, pp. 12-17.

4. Kapp, R. H., Discussion of Reference (3), Engineering Journal, AISC, Vol. 11, No. 3, 1974, p. 80.

5. Kapp, R. H., "Yield Line Analysis of a Web Connection in Direct Tension," Engineering Journal, AISC, 1974, pp. 38-41.

6. Csnerak, S. F., "Evaluation of the Strength of Column Web Connections," A Report Submitted to the Department of Civil Engineering in Partial Fulfillment of the Requirements for the Degree of Master of Science, Clemson University, February, 1976.

7. Zienkiewicz, O. C. and Cheung, Y. K., "The Finite Element Method for Analysis of Elastic Isotropic and Orthotropic Slabs," Proceedings, Inst. Civil Eng., Vol. 28, 1964, pp. 471-488.

8. Hill, R., The Mathematical Theory of Plasticity, Oxford University Press, London, 1950.

9. Hodge, P. G., Jr., Limit Analysis of Rotationally Symmetric Plates and Shells, Prentice-Hall, New Jersey, 1963.

10. Dubey, R. N., "Incremental Theory of Plasticity: New Approach," Mech. Res. Comm., Vol. 4, 1977, pp. 35-39.

11. Yamada, Y., et al., "Plastic Stress-Strain Matrix and Its Application for the Solution of Elastic-Plastic Problems by Finite Element Method," Int. J. Mech. Sci., Vol. 10, 1968, pp. 343-354.

12. Shoeb, N. A. and Schnobrich, W. C., "Analysis of Elasto-Plastic Shell Structures," Civil Eng. Studies, Structural Research Series No. 324, University of Illinois, August, 1967.

13. Ang, A. H. and Lopez, L. A., "Discrete Model Analysis of Elastic-Plastic Plates," J. Eng. Mech., ASCE, Vol. 94, No. EM1, 1968, pp. 271-293.

14. Marcal, P. V. and Mallett, R. H., "Elastic-Plastic Analysis of Flat Plates by the Finite Element Method," Paper No. 68-WA/ PVP-10, ASME Winter Annual Meeting, New York, 1968.

15. Wegmuller, A. W., "Full Range Analysis of Eccentrically Stiffened Plates," J. Struc. Div., ASCE, Vol. 100, No. ST1, 1974, pp. 143-159.

16. Marcal, P. V., "A Stiffness Method for Elastic-Plastic Problems," Int. J. Mech. Sci., Vol. 7, 1965, p. 229-238.

17. Specification for the Design, Fabrication and Erection of Structural Steel for Buildings, American Institute of Steel Construction, New York, 1973.

18. Weisgerber, F. E. and Anand, S. C., "Interpolative Versus Iterative Solution Schemes for Tresca Yield Condition in Elastic-Plastic Finite Element Analysis," Int. J. Num. Meth. Eng., Vol. 12, 1978, pp. 765-777.

19. Martin, H. C., Introduction to Matrix Methods of Structural Analysis, McGraw-Hill, New York, 1966.